Feedback control strategies for quadrotor-type aerial robots: a survey

Necdet Sinan Özbek[1,2], Mert Önkol[3] and Mehmet Önder Efe[4]

Abstract

Control of aerial robots is a popular research field as applications with different payloads lead to a variety of flight missions. Quadrotor-type unmanned systems are one such example considered in this paper. The performance in any flight experiment depends strictly on the chosen feedback control scheme, which is the core issue addressed in the paper. A number of approaches have been reported in the literature and this paper presents a survey of these schemes with an in-depth discussion of recent research outcomes. A detailed performance evaluation of the controllers, namely proportional-integral-derivative control, sliding mode control, backstepping control, feedback linearization-based control and fuzzy control schemes, are presented. Due to the popularity of the quadrotor-type aerial vehicles, the contribution of the current work is to provide an in-depth guide to the autopilot designers of quadrotor-type unmanned aerial vehicles.

Introduction

The advances in sensing technology, communication networks, embedded computing devices and information processing platforms have made it possible to design high-performance control systems. The enhancements in these areas have been essential for the development of control systems, such as those applied to aviation systems, unmanned aerial vehicles (UAVs), highly manoeuvrable aircrafts, energy-efficient and safe vehicles, smart phones, aerospace systems, autonomous robots and further applications across various industrial sectors (Samad and Annaswamy, 2011).

Roughly speaking, the UAVs are aircraft systems that are operated without a human pilot on board and they can be autonomous or remotely controlled. UAVs have a great number of the advantages compared to manned aerial vehicles, particularly for missions that are beyond the limitations of human endurance. Furthermore, they have noteworthy properties, such as the ability of being invisible to radars, which provides critically important surveillance information. Due to these mentioned advantages, the popularity of UAVs has grown tremendously in numerous missions, including industrial, academic, governmental, military and civilian. Therefore, parallel to this, the importance of autopilot and low-level control has become the central issue of UAV prototyping.

A quadrotor rotorcraft, which is basically a vertical take-off and landing (VTOL) aerial robot with a cross-directional rigid body configuration (Castillo, 2004), is a widely used benchmark system for robotics research. The structure of the quadrotor provides a number of advantages compared to traditional helicopters and fixed-wing aircrafts. The thrust force, for instance, can be easily adjusted by commuting the speed of each rotor; in this way complicated variable pitch components can be avoided. In addition, rotors can balance each other's torques by means of the counter-rotating structure; thus, this structure does not need a tail rotor. Furthermore, rapid manoeuvrability, easy maintainability, low-cost manufacturability with reduced mechanical complexity and stable hovering capability above a target, make it a well-suited platform for various tasks, such as small area monitoring, surveillance, damage assessment, mapping after disasters, detection in restricted terrains and reconnaissance, as well as search and rescue missions (Tomic et al., 2012). For such purposes, a considerable number of quadrotors having a variety of structures and properties have been manufactured in various research projects, such as Castillo et al. (2005), Hoffman et al. (2004), Guenard et al. (2008), Bouabdullah (2007) and Meier et al. (2011), and some recent types of quadrotors with tilting propellers and new configurations have been constructed by Oner et al. (2008), Sanchez et al. (2008), Meier et al. (2011), Senkul and Altuğ (2013), Driessen and Pounds (2013),

[1]Department of Electrical and Electronics Engineering, Adana Science and Technology University, Turkey
[2]Department of Electrical and Electronics Engineering, Çukurova University, Turkey
[3]Digicraft Mühendislik ve Bilgi Teknolojileri, Turkey
[4]Department of Computer Engineering, Hacettepe University, Turkey

Corresponding author:
Necdet Sinan Özbek, Department of Electrical and Electronics Engineering, Adana Science and Technology University, 01180 Adana, Turkey.
Email: nozbek@adanabtu.edu.tr

Ryll et al. (2014) and Wu et al. (2014). Some results considering the stability and performance analysis are discussed by Toledo et al. (2015); parallel to this study, Kalantari and Spenko (2015) presents modelling and performance assessment of a hybrid terrestrial/aerial quadrotor.

Recently, quadrotors have been used in cooperative control and multi-agent applications to explore unknown environments in order to maintain long-term and distributed surveillance and search and rescue missions, which have benefited extensively from the swarm technology. The widespread applications and incredible efficiency of the quadrotor-type aerial robots for a variety of tasks motivate researchers to investigate and assess control techniques, which play a crucial role in the autopilot's performance. Towards this goal, robustness against disturbances, measurement errors and unmodelled dynamics are addressed in the recent work of Hua et al. (2013). The key difficulty of designing a controller for a quadrotor system is the presence of highly nonlinear and inextricably intertwined system dynamics with an unstable and underactuated nature, which are difficult to handle solely by linear control solutions. These are stated in a number of recent researches (Bouabdallah and Siegwart, 2007; Castillo et al., 2004, 2005; Lozano, 2010; Mahony and Kumar, 2012; Pounds, 2008) in the context of quadrotor control design. Newly published works also perform stability analysis of the quadrotors with the designed controllers (Gupte et al., 2012; Hua et al., 2009, 2013), and address modelling and parameter estimation issues in quadrotor design (Mahony and Kumar, 2012). Recent research results for quadrotor modelling and quadrotor parameter identification are presented by Zhang et al. (2014). A survey for categorization of small aerial vehicles based on the system identification approaches is presented by Hoffer et al. (2014) and Cai et al. (2014). However, it is still necessary to elucidate many other issues, before all the benefits of utilizing a quadrotor can be harvested.

The motivation of this work stems from the necessity of analysing existing, mostly recent, controller designs and applications to quadrotors to express advantages and disadvantages of the each controller, in order to point out directions for researchers interested in controller design for quadrotors. With this motivation in mind, a performance assessment is presented via results of several illustrations and numerical measures, with complementary comments on the advantages and drawbacks of the each strategy. Particular attention is paid to the tracking precision, applicability of control signals, quality of the transient response and energy efficiency of each control strategy with respect to some performance criteria, such as maximum absolute error (MAE), error variance (EV), integral absolute error (IAE), integral squared error (ISE), integral time squared error (ITSE) and integral squared control input (ISCI).

This paper is organized as follows: the second section presents the derivation of the dynamical equations governing the quadrotor motion. The third section discusses the control strategies with the relevant literature, in particular covering the recent research outcomes. As a starting case, the proportional-integral-derivative (PID) loop is first discussed, then a number of nonlinear control strategies, namely the backstepping (BS) control, sliding mode control (SMC), feedback linearization (FBL)-based control and fuzzy control implementations, for the quadrotors are addressed. For each approach, a discussion on the effect of the chosen parameters is given and simulation results according to several performance metrics are rigorously presented with the help of tabulated observations. The fourth section presents a comparative discussion for each controller. Finally, the last section summarizes the contributions and conclusions of the paper.

Dynamic modelling of the quadrotor

The dynamic model has an important role in understanding the behaviour of the quadrotor UAV. Since the functional details embodying the plant dynamics are inputs to the controller design procedure, it is essential to obtain an accurate dynamic model of the vehicle (Bouabdallah 2007; Bouabdallah et al., 2004a; Elsamanty et al., 2013; Kim et al., 2010; Pounds, 2008; Zhang et al., 2014).

The quadrotor system consists of two pairs of counter-rotating rotors, which eliminate anti-torque occurring due to the undesired yaw motion produced by the rotors (Mahony et al., 2012). Referring to Figure 1, the propeller pair 1 and 3 rotates in the counter direction with respect to propeller pair 2 and 4. Roll motion around the x-axis can be obtained by inversely and proportionally changing the angular velocities of rotors 2 and 4, and similarly pitch motion can be made possible by inversely and proportionally changing the angular velocities of rotors 1 and 3 where the difference of the four propellers' velocities yields yaw motion about the z-axis. The coordinates and structure of the quadrotor are depicted in Figure 1.

In order to obtain the model parameters of the quadrotor, a number of assumptions are made. In the derivation of the model, Euler–Lagrange formalism or Newton–Euler formalism are considered frequently (Bouabdullah et al., 2004a; Castillo et al., 2005; Hamel et al., 2002; Mian and Daobo, 2008; Zhang et al., 2014). It should be pointed out that the Newton–Euler method is straightforward and is applied in this paper. Nevertheless, the results of both methods capture the same physical reality. The developed model is dependent upon the known constants, any uncertainty on which can subsequently be handled via system identification methods (Bergamasco and Lovera, 2014; Gremillion, 2010; Zhang et al., 2014). Recent results for the categorization of the system identification methods are reviewed by Hoffer et al. (2014). However, it should be noted that there are relatively few results for the identification of the multi-rotors with the system identification approaches, since identifying the unstable dynamics of the quadrotor with open-loop approaches is impractical (Zhang et al., 2014).

During the derivation of the dynamical model of the quadrotor, we consider the assumptions listed below:

1. the structure of the quadrotor is symmetrical and rigid;
2. the ground effect is neglected;
3. the propellers are considered as rigid;
4. thrust and drag forces are proportional to squares of the propellers' angular velocities;
5. the centre of mass and the origin of the body fixed frame are coinciding.
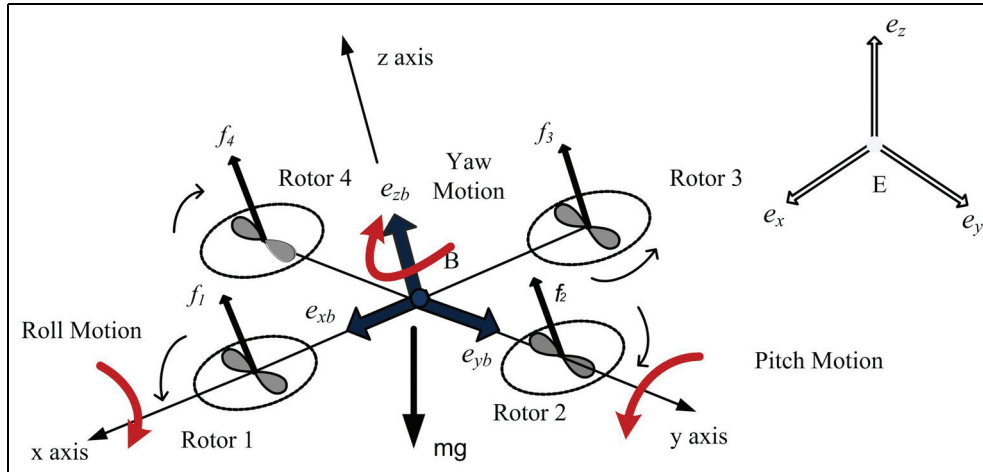
Figure 1. The structure of the quadrotor unmanned aerial vehicle.

The dynamics that emerge due to the extraction of the external force to body of the quadrotor can be depicted on the body fixed coordinate frame and the following representation is obtained to model translational and rotational motions:

$$\begin{bmatrix} m\mathbf{I}_{3\times3} & 0 \\ 0 & \mathbf{I} \end{bmatrix} \begin{bmatrix} \dot{\mathbf{v}} \\ \dot{\boldsymbol{\omega}} \end{bmatrix} + \begin{bmatrix} \boldsymbol{\omega} \times m\mathbf{v} \\ \boldsymbol{\omega} \times \mathbf{I}\boldsymbol{\omega} \end{bmatrix} = \begin{bmatrix} \mathbf{F} \\ \boldsymbol{\tau} \end{bmatrix} \quad (1)$$

In Figure 1, frame E denotes the earth fixed frame, B denotes the body fixed frame and R is a transformation matrix from B to E. In (1), $I \in R^{3\times3}$, $\boldsymbol{\omega}$ is the body angular velocity and $\mathbf{v}$ is the body linear velocity vector. The dynamics in (1) can explicitly be written as below:

$$\dot{\boldsymbol{\zeta}} = \mathbf{v} \quad (2)$$

and

$$\dot{\mathbf{v}} = -g\mathbf{e}_z + \frac{1}{m}TR\mathbf{e}_z \quad (3)$$

$$\mathbf{I}\dot{\boldsymbol{\omega}} = -\boldsymbol{\omega} \times \mathbf{I}\boldsymbol{\omega} + \boldsymbol{\tau}_f - \boldsymbol{\tau}_g \quad (4)$$

$$\text{sk}(\boldsymbol{\omega}) = R^T\dot{R} \quad (5)$$

where $\boldsymbol{\zeta} = (x, y, z)^T$ represents the position of the body fixed coordinate frame with respect to the earth fixed coordinate frame, $\mathbf{v}$ represents the linear velocities in the earth fixed frame, $\mathbf{T}$ is the thrust force produced by propellers, g is the gravitational acceleration and $\mathbf{e}_z$ stands for the z component of the unit vector. It is obvious from (3) that only the existence of $\mathbf{e}_z$ proves that thrust force is in the direction of z. R, which is a function of angular quantities and described in (6), is used to map the forces in the body fixed frame to the earth fixed frame. The angular motion of the vehicle is described in (4), where applied torques on the quadrotor cause rotational motion. A well-known matrix in model derivation is the skew symmetric matrix, which is the derivative of rotation matrix R given by (6):

$$R(\phi, \theta, \psi) = \begin{bmatrix} c\psi c\theta & c\psi s\theta s\phi - s\psi c\phi & c\psi s\theta c\phi + s\psi s\phi \\ s\psi c\theta & s\psi s\theta s\phi + c\psi c\phi & s\psi s\theta c\phi - s\phi c\psi \\ -s\theta & c\theta s\phi & c\theta c\phi \end{bmatrix} \quad (6)$$

where $c\theta$ is $\cos\theta$ and $s\theta$ is $\sin\theta$. One can modify (3) and obtain the representation in (7):

$$\mathbf{F}_b = -mg\mathbf{E}_z + R\sum_{i=1}^{4}\mathbf{T}_i \quad (7)$$

The above representation is required to get the translational dynamic equations of the quadrotor, where the explicit form of the expression can be written as below:

$$\mathbf{F}_b = -\begin{bmatrix} 0 \\ 0 \\ m\mathbf{g} \end{bmatrix}$$
$$+ \begin{bmatrix} c\psi c\theta & c\psi s\theta s\phi - s\psi c\phi & c\psi s\theta c\phi + s\psi s\phi \\ s\psi c\theta & s\psi s\theta s\phi + c\psi c\phi & s\psi s\theta c\phi - s\phi c\psi \\ -s\theta & c\theta s\phi & c\theta c\phi \end{bmatrix}$$
$$\begin{bmatrix} 0 \\ 0 \\ \sum_{i=1}^{4}\mathbf{T}_i \end{bmatrix} \quad (8)$$

The dynamics depicting the linear motion of the vehicle is described in (9)–(11) where m is the mass of the quadrotor:

$$\ddot{x} = (\cos\phi\sin\theta\cos\psi + \sin\phi\sin\psi)\frac{1}{m}U_1 \quad (9)$$

$$\ddot{y} = (\cos\phi\sin\theta\sin\psi - \sin\phi\cos\psi)\frac{1}{m}U_1 \quad (10)$$

$$\ddot{z} = -g + (\cos\phi\cos\theta)\frac{1}{m}U_1 \quad (11)$$

Regarding the angular dynamics, the body velocities are transformed to those expressed by the Euler angles by

considering rotation ψ about the z-axis, rotation θ about the y-axis and rotation ϕ about the x-axis. This yields the following matrix equality:

$$\begin{bmatrix} \dot{\phi} \\ \dot{\theta} \\ \dot{\psi} \end{bmatrix} = \begin{bmatrix} 1 & \sin\phi\tan\theta & \cos\phi\tan\theta \\ 0 & \cos\phi & -\sin\phi \\ 0 & \sin\phi\sec\theta & \cos\phi\sec\theta \end{bmatrix} \begin{bmatrix} \mathbf{p} \\ \mathbf{q} \\ \mathbf{r} \end{bmatrix} \quad (12)$$

$\omega := \{\mathbf{p}, \mathbf{q}, \mathbf{r}\}$ stands for the angular velocities and quadrotor motion lets us use small angle approximation (SAA). The gyroscopic effect caused by the rotation of the rigid body is described as in (13):

$$-\omega \times I\omega = [(I_{yy} - I_{zz})\dot{\theta}\dot{\psi} \;\; (I_{xx} - I_{yy})\dot{\theta}\dot{\phi} \;\; (I_{zz} - I_{xx})\dot{\phi}\dot{\psi}]^T \quad (13)$$

where I_{xx}, I_{yy} and I_{zz} are inertias of the body due to rotations around the x, y and z-axes, respectively. The change in the orientation of propellers yields gyroscopic torque, which is defined as

$$\tau_g := \sum_{i=1}^{4} (\Omega \times J_r)(-1)^{i+1}\omega_i e_z \quad (14)$$

where Ω is the propeller angular speed and J_r is the propeller inertia. The vector of control moments denoted by τ_a is given in (15):

$$\tau_a = [\tau_{roll} \;\; \tau_{pitch} \;\; \tau_{yaw}]^T = [l(T_4 - T_2) \;\; l(T_1 - T_3) \\ -Q_1 + Q_2 - Q_3 + Q_4]^T \quad (15)$$

With these terms, the angular dynamics can be written as in (16)–(18):

$$\ddot{\phi} = \dot{\theta}\dot{\psi}\left[\frac{I_{yy} - I_{zz}}{I_{xx}}\right] - \frac{J_r}{I_{xx}}\dot{\theta}\Omega_r + \frac{l}{I_{xx}}U_2 \quad (16)$$

$$\ddot{\theta} = \dot{\phi}\dot{\psi}\left[\frac{I_{zz} - I_{xx}}{I_{yy}}\right] + \frac{J_r}{I_{yy}}\dot{\phi}\Omega_r + \frac{l}{I_{yy}}U_3 \quad (17)$$

$$\ddot{\psi} = \dot{\theta}\dot{\phi}\left[\frac{I_{xx} - I_{yy}}{I_{zz}}\right] + \frac{1}{I_{zz}}U_4 \quad (18)$$

The control inputs seen in the dynamical model are defined as in (19)–(22), where Ω_i is the angular speed of the ith rotor and Ω_r is defined as in (23):

$$U_1 = b(\Omega_1^2 + \Omega_2^2 + \Omega_3^2 + \Omega_4^2) \quad (19)$$

$$U_2 = M_x = b(\Omega_4^2 - \Omega_2^2) \quad (20)$$

$$U_3 = M_y = b(\Omega_3^2 - \Omega_1^2) \quad (21)$$

$$U_4 = M_z = d(\Omega_1^2 + \Omega_3^2 - \Omega_2^2 - \Omega_4^2) \quad (22)$$

$$\Omega_r = \Omega_1 - \Omega_2 + \Omega_3 - \Omega_4 \quad (23)$$

The entire system dynamics can be written as

$$\dot{X} = f(X, U) \quad (24)$$

Table 1. Physical parameters of the quadrotor system.

Total weight of the vehicle	m	0.800 kg
Gravitational acceleration	g	9.81 kg/m^2
Arm length of the vehicle	l	0.3 m
Moment of inertia along x-axis	I_{xx}	15.67×10^{-3} kgm^2
Moment of inertia along y-axis	I_{yy}	15.67×10^{-3} kgm^2
Moment of inertia along z-axis	I_{zz}	28.34×10^{-3} kgm^2
Thrust factor	b	192.32×10^{-7} Ns^2
Drag factor	d	4.003×10^{-7} Nms^2
Propeller inertia	J_r	6.01×10^{-5} kgm^2

where X denotes the state vector and U is the input vector. The content of the state vector is given in (25):

$$X = [\phi \;\; \dot{\phi} \;\; \theta \;\; \dot{\theta} \;\; \psi \;\; \dot{\psi} \;\; x \;\; \dot{x} \;\; y \;\; \dot{y} \;\; z \;\; \dot{z}]^T \quad (25)$$

In order to write $f(X, U)$ compactly, define the state variables as $x_1 = \phi, x_2 = \dot{\phi}, x_3 = \theta, x_4 = \dot{\theta}, x_5 = \psi, x_6 = \dot{\psi}, x_7 = x, x_8 = \dot{x}, x_9 = y, x_{10} = \dot{y}, x_{11} = z, x_{12} = \dot{z}$, then we have

$$f(X, U) = \begin{bmatrix} x_2 \\ p_1 x_4 x_6 - p_2 x_4 \Omega_d + p_3 U_2 \\ x_4 \\ p_4 x_2 x_6 + p_5 x_2 \Omega_d + p_6 U_3 \\ x_6 \\ p_7 x_4 x_2 + p_8 U_4 \\ x_8 \\ (c_\phi s_\theta c_\psi + s_\phi s_\psi)\frac{1}{m}U_1 \\ x_{10} \\ (c_\phi s_\theta s_\psi + s_\phi c_\psi)\frac{1}{m}U_1 \\ x_{12} \\ -g + (c_\phi c_\theta)\frac{1}{m}U_1 \end{bmatrix} \quad (26)$$

where $p_1 = (I_{yy} - I_{zz})/I_{xx}$, $p_2 = J_r/I_{xx}$, $p_3 = l/I_{xx}$, $p_4 = (I_{zz} - I_{xx})/I_{yy}$, $p_5 = J_r/I_{yy}$, $p_6 = l/I_{yy}$, $p_7 = (I_{xx} - I_{yy})/I_{zz}$, $p_8 = 1/I_{zz}$. The physical parameters of the system are given in Table 1.

Control strategies

An unmanned aerial robot needs a robust control system to alleviate the adverse effects of parametric and non-parametric uncertainties, unmeasured dynamics and atmospheric disturbances, such as wind and turbulence (Lugue-Vega et al., 2012). Essentially, the quadrotor system has six degrees of freedom (DOFs), while it has only four control inputs consisting of thrust and the three rotational torque inputs, and this makes it an underactuated system (Dierks and Jagannathan, 2009). During the last decade, design and implementation of the flight controller for such nonlinear underactuated systems has drawn considerable interest. Until recently, designing a control algorithm for the quadrotor UAV achieving the requirements of an autonomous flight was a significant challenge, and therefore, to handle this problem, the control engineering framework offers elegant solutions based on bounded control, quadratic optimization, constrained finite-time optimal control, hard boundary switching laws (SMC) or soft boundary laws, such as fuzzy set theory and predictive control (Özbek and Efe, 2010). It is worth mentioning that the
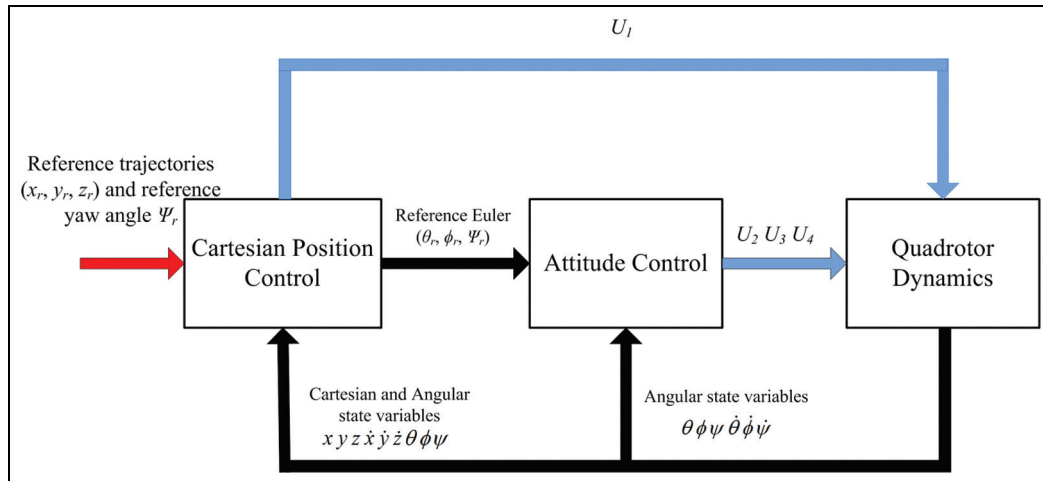
Figure 2. The control structure of the quadrotor.

synergic combination of different approaches can provide satisfactory results in both the attitude stabilization (Derafa et al., 2012; Lugue-Vega et al., 2012) and tracking control (Bouabdallah and Siegwart, 2005, 2007; Madani and Benallegue, 2006, 2007).

The dynamics of a quadrotor exhibits distinct characteristics for different flight missions, such as VTOL, horizontal flight, aggressive manoeuvres and hovering mode involved in the execution of the flight task. Up to now, the hovering mode has attracted significant attention, probably owing to the fact that hovering is one of the most important regimes (Zhang et al., 2014). In the case of hovering and forward flight with low velocity, the simplistic assumptions, which are often ignored due to known aerodynamic effects of aircraft, are approximately reasonable. However, in recent applications such as acrobatic flight (Mellinger et al., 2014), dancing with music (Schoelling et al., 2010) and multi-flips (Korpela et al., 2012; Lupashin et al., 2010), the quadrotor needs high manoeuvrability. Unfortunately, in this case, the simplistic assumptions are no more suitable as the stability of the system is significantly fragile because of the presence of additional aerodynamic forces, moments and ground effects that are not negligible.

The structure of the control system established for every quadrotor control application is as depicted in Figure 2, where the outer loop determines the necessary Euler angles and inner loop forces to track these angles to move the vehicle towards the desired Cartesian position. According to the figure, the control input for the translational dynamics is denoted by U_1. The control inputs influencing the attitude of the vehicle are U_2 for the roll axis, U_3 for the pitch axis and U_4 for the yaw axis (Efe, 2011a). The fundamental issue is to keep the quadrotor at a desired altitude; hence, $U_1 = m(U_z + g)/\cos\phi\cos\theta$ is chosen to linearize the z dynamics. With such a U_1, it yields $\ddot{z} = U_z$ with U_z is to be determined later on.

In this study, the effects of the user-defined controller parameters are investigated in detail. Clearly, the number of alternatives is infinitely many but the studied parameter sets describe the dynamically different regimes and their effects on the measurable performance metrics. To measure the performance of the designed controllers, MAE, EV and computational complexity as primary measures are considered. Further, the ISCI given by $ISCI = \int U_i^2(t)\mathrm{d}t$, the integral of the absolute error given by $IAE = \int |e(t)|\mathrm{d}t$ and the integral of the squared error given by $ISE = \int e^2(t)\mathrm{d}t$ are studied to compare the performance of the chosen approaches (Seborg et al., 1989).

The two-step parameter tuning strategy can be explained as follows: in the first step, special attention is paid to the stabilization of fast dynamics, which corresponds to inner control loop. Thus, the controller, which compensates the rotational dynamics, is adjusted until a satisfied response is obtained. Secondly, translational dynamics are considered, which involves the outer feedback loop, as seen in Figure 2. The parameters associated with the translational dynamics are tuned to obtain a satisfactory behaviour in the Cartesian space (Carillo et al., 2012).

A review of linear control strategies for quadrotor control

Linear control strategies, which are based on linear approximations of the system dynamics around desired operating conditions, are especially preferred in autopilot applications, where the angle of attack over the nominal flight envelop is small (Hua et al., 2013). Successful applications are reported by Bouabdallah et al. (2004a, 2004b), Pounds (2008), Hoffmann et al. (2004, 2011). Among the cited works, Pounds (2008) shows that linear controllers successfully stabilize the prototype X-4 Flyer in the presence of step disturbances. PID and linear quadratic regulator (LQR)-based methods have been studied by Bouabdallah et al. (2004b) with an application to the OS4 platform. This study presents the capability of the PID controller to handle attitude stabilization problem, and shows that the LQR controller provides average-quality results in the presence of minor perturbations

and model imperfections. A further LQR approach, which optimizes the controller gains, is presented by Cowling et al. (2007).

In addition, an energy-efficient autonomous flight scenario is highlighted by Gurdan et al. (2007). Stabilization and altitude tracking of a quadrotor using lifting operators is addressed by Toledo et al. (2009). Belkheiri et al. (2012) propose linearization-based control algorithms to solve the stabilization problem of the quadrotor. In that work, the tangent linearization method is employed and a linear model of the system is generated where decentralized and centralized LQR methods are applied. A gain scheduling-based LQR control strategy is highlighted by Reyes-Valeria et al. (2013). In that study, a unit quaternion approach is employed to control the attitude behaviour of the quadrotor. Tayebi and McGilvray (2006) propose a PD^2 feedback controller based on the quaternion model, which is generally employed to control the rigid body dynamics. Furthermore, it was indicated that exponential stability can be guaranteed by means of the compensated Coriolis and gyroscopic torques, whereas a well-established PD control scheme without compensated Coriolis and gyroscopic torques can provide asymptotic stability (Lee et al., 2009). Both linear and nonlinear control strategies based on dual camera visual feedback are presented by Altuğ et al. (2003).

Moreover, Erginer and Altuğ (2007) present a PD controller using visual feedback. Voos (2009) propose a state-dependent Riccatti equation-based control strategy using the SAA in order to obtain the desired angular position, which is a prerequisite for velocity tracking. Another study combining conventional PID and LQ control to constitute a hybrid control strategy was discussed by Orsag et al. (2010). A formulation based on nonlinear programming is proposed to give optimal control of a hovering quadrotor (Lai et al., 2006). In that study, the sampling period is considered as a variable in the optimization process. Moreover, genetic algorithms are employed to present the feasibility of the proposed method. The finite-time output feedback problem is elaborated by Zhang et al. (2012). In that study, a finite-time state feedback controller is proposed and a finite-time-stable observer is developed to estimate the unmeasurable states. The reported feedback control strategy is developed with an open-loop controller that enables the quadrotor to perform more aggressive manoeuvres than the standard counterparts. Li and Li (2011) present dynamic modelling and a PID control scheme for a quadrotor. In another study, a linear model predictive control (LMPC) strategy is implemented on a Qball-X4 platform in order to follow a circular path (Iskandarani et al., 2013). Sadeghzadeh et al. (2012) propose a gain-scheduled PID controller for active fault-tolerant control for a quadrotor in the presence of actuator faults. Araar and Aouf (2014) address two fully linear techniques based on optimal control theory. In the first approach, a LQ servo controller, which is based on the L$_2$ norm, is presented. The second approach optimizes the L$_\infty$ norm and is designed using the H$_\infty$ control approach. As one of the recent trending topics of control society, event-triggered attitude stabilization with quaternion-based feedback is presented by Guerrero-Castellanos et al. (2013). On the other hand, event-driven PID control of a quadrotor is addressed by Wang et al. (2011), and a performance comparison of event-driven and time-driven methods is presented by Wang et al. (2013). However, it is worth mentioning that in the case of linear controllers, one can only guarantee stability of the closed-loop system for small regions around the equilibrium point. Due to the popularity of the PID control scheme, we present a case study of the PID approach for quadrotor control.

A case study: PID control for the quadrotor. In order to design the PID controllers for the quadrotor, nonlinear rotational dynamics of the quadrotor are linearized around zero, which results in the following linear representation, with s being the Laplace variable:

$$\phi(s) = \frac{1}{s^2} \frac{l}{I_{xx}} U_2(s) \tag{27}$$

$$\theta(s) = \frac{1}{s^2} \frac{l}{I_{yy}} U_3(s) \tag{28}$$

$$\psi(s) = \frac{1}{s^2} \frac{1}{I_{zz}} U_4(s) \tag{29}$$

The choice of U_1 is as described previously. It is proposed to adjust the gains to reach an acceptable level of tracking performance in Euler angles. The PID controller for each subdynamics is given as follows:

$$U_2 = K_{p\phi}(\phi_d - \phi) + K_{i\phi} \int (\phi_d - \phi)\mathrm{d}t + K_{d\phi}\dot{\phi} \tag{30}$$

$$U_3 = K_{p\theta}(\theta_r - \theta) + K_{i\theta} \int (\theta_r - \theta)\mathrm{d}t - K_{d\theta}\dot{\theta} \tag{31}$$

$$U_4 = K_{p\psi}(\psi_r - \psi) + K_{i\psi} \int (\psi_r - \psi)\mathrm{d}t - K_{d\psi}\dot{\psi} \tag{32}$$

where the desired roll, pitch and yaw angles are shown with a subscript d, and the problem here is to choose the PID gains for each subsystem.

Investigating the effects of the PID control parameters on control performance and design specifications. The PID controller is the most preferable control strategy because of its simplicity. The controller gains K_p, K_i and K_d are determined using traditional controller design approaches that exploit a linearized model around a desired operating point.

In this study, the system has been simulated for two different sets of K_p, K_i, K_d values. The tracking errors and control signals have been recorded in each case. In the first set, the coefficients for the roll and pitch dynamics are chosen as $K_{p\phi} = K_{p\theta} = 1$, $K_{i\phi} = K_{i\theta} = 0.13$, $K_{d\phi} = K_{d\theta} = 0.66$, and for the yaw dynamics, $K_{p\Psi} = 0.1$, $K_{i\Psi} = 0.013$, $K_{d\Psi} = 0.066$ are chosen. The roll and pitch controller coefficients for the second set are $K_{p\phi} = 1.55$, $K_{i\phi} = 0.17$, $K_{d\phi} = 0.76$ and for the yaw controller are $K_{p\Psi} = 0.02$, $K_{i\Psi} = 0.01$, $K_{d\Psi} = 0.01$. Measurement noise with a very small variance is added to the angular quantities to make the simulations more realistic. The parameters given above are obtained through a simple

Table 2. Measured performances of the proportional-integral-derivative controller for two different parameter sets.

Criterion	Set-1			Set-2		
	Pitch (θ)	Roll (φ)	Yaw (ψ)	Pitch (θ)	Roll (φ)	Yaw (ψ)
IAE	7.7083	4.2266	4.5995	7.14893	3.76810	4.5526
MAE	0.5228	0.3682	0.3683	1.1732	0.3647	0.3681
ISE	1.467	0.1387	0.1571	1.1648	0.1478	0.1574
ITSE	34.7876	16.8805	13.2593	28.9148	10.2766	13.2560
EV	0.0011	0.0027743	0.000314	0.0023	0.000295	0.0003147

IAE: integral absolute error; MAE: maximum absolute error; ISE: integral squared error; ITSE: integral time squared error; EV: error variance.

Table 3. Measured integral squared control input (ISCI) and control signal variances of the proportional-integral-derivative controller for two different parameter sets.

Criterion		Control inputs for Set-1	Controller inputs for Set-2
ISCI	U_1	2.9734 e + 04	2.9818 e + 04
	U_2	0.2364	0.6695
	U_3	0.7602	2.4962
	U_4	0.0022	0.0023
Control input variance	U_1	0.1847	0.2495
	U_2	4.7280e-04	0.0013
	U_3	0.0015	0.0050
	U_4	4.3731e-06	4.6767e-06

Figure 3. The tracking results for the proportional-integral-derivative control technique for Set-1.

design for the linear system and trial-and-error-based refinement on the nonlinear model.

The relative importance of the tracking performance and the amount of control effort play a central role in the selection of the controller gains. The designer can observe the changes in the expended control effort and tracking error when the controller parameters are changed. Eventually a good performing set can be fixed after a refinement process. In this study, controller performance evaluation is performed in the light of MAE, EV and IAE as performance criteria.

Expectedly, the variation in each controller coefficient has an effect on the stability of the closed loop and the performance of the vehicle. For example, proportional gain increases the manoeuvrability of the vehicle. However, the system with a large K_p is much more sensitive and reactive to angular change, thus the larger the K_p the larger the overshoot. The integral term removes the steady-state deviations from the desired trajectory but it slows down the response. On the other hand, the derivative term speeds up the system response, yet the system becomes sensitive to noise or sudden disturbances. Generally speaking, for aggressive flights, it is better to choose larger proportional and derivative coefficients and smaller integral coefficient. Conversely, for smooth flight regimes, the system needs smaller proportional and derivative coefficients.

The results of the PID scheme for choosing control parameters are shown in Figures 3–6, where it is seen that the attitude stabilization is obtained with satisfactory precision. Tables 2 and 3 summarize the system performance for the
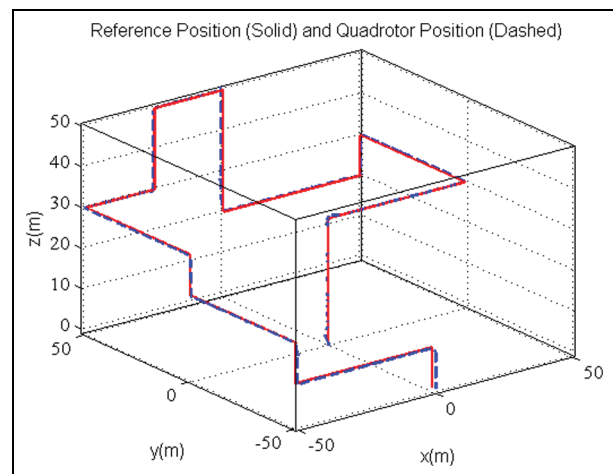
two sets of controller parameters. Initial errors are compensated fairly quickly and the controller produces fairly smooth control signals having reasonable magnitudes. The smoothness of the control signals has a vital importance on system performance due to the possible physical restrictions on the actuation system. Even though the reference trajectory is a discontinuous one, the demonstrated control strategy satisfactorily enforces the quadrotor to the desired altitude and attitude position in finite time, as shown in Figures 3–5.

Nonlinear control strategies

Recently, there have been various strategies devoted to designing nonlinear controllers (Bouabdallah, 2007; Bouabdallah and Siegwart, 2007; Castillo et al., 2006; Efe, 2007; Madani and Benallegue, 2006) that may overcome important difficulties, such as parametric uncertainties, aerodynamic disturbances, variations in the mass of the vehicle or actuator saturations, measurement errors, etc. The majority of the nonlinear design methods are based on Lyapunov approaches (Slotine and Li, 1991). In the following, we present some of the nonlinear control strategies for the quadrotor aerial robot with an in-depth review of the relevant literature.

A case study: feedback linearization technique for the quadrotor. The central idea of FBL is to algebraically
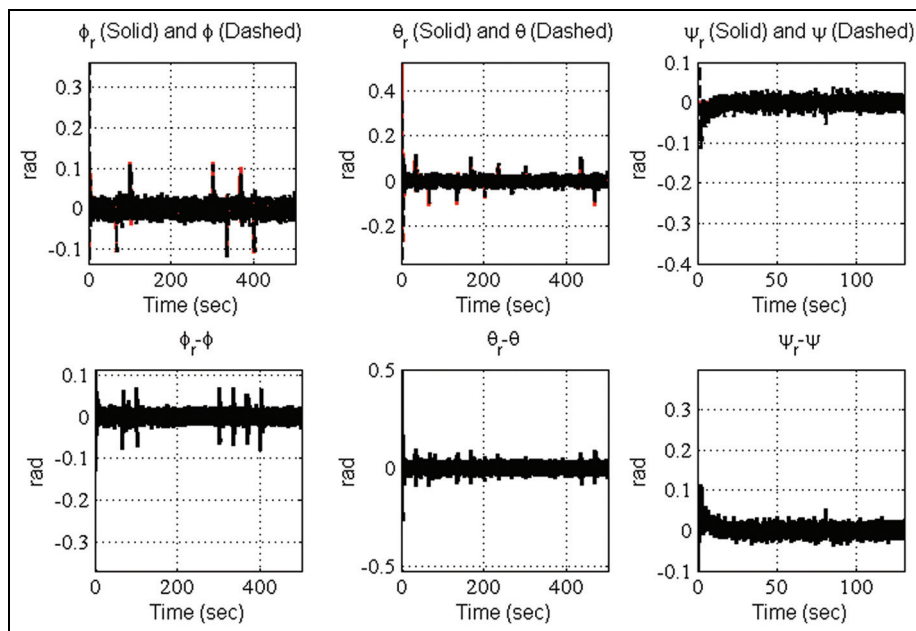
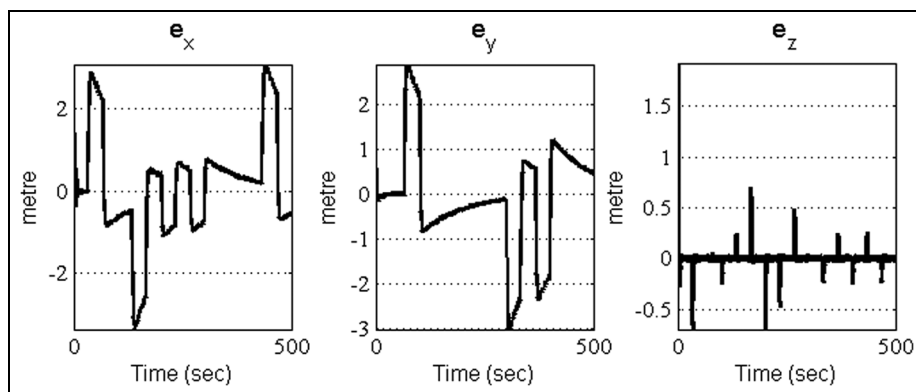**Figure 4.** Results for the Euler angles (attitude) for Set-1.

Figure 5. Proportional-integral-derivative control results for the Cartesian space variables for Set-1.

transform a given nonlinear system dynamics to a linear dynamical form by an appropriate feedback law. The next phase of the design is to obtain linear control laws as the system under scrutiny has been linearized. In the FBL scheme, the control law is obtained via an exact state transformation rather than by linear approximation of the states (Gee et al., 1998). FBL control operates smoothly in the cases that all the system parameters are well defined; therefore, it has a remarkable handicap when the nonlinear equivalent dynamic formulation contains uncertainties. Some works are proposed to overcome the aforementioned problem by combining intelligent methods, as presented by Mukherjee and Waslander (2012). Voos (2009) introduce a FBL control scheme based on decomposition into a nested structure, where it is easy to implement the method on a microcontroller. Mian and Daobo (2008) propose a control strategy that combines FBL and BS control schemes. In that study, the FBL method is

employed for the translational motion control and the BS controller is employed for the rotational (attitude) motion control of the quadrotor. Lee et al. (2009) propose FBL and adaptive sliding mode-based control schemes where, firstly, a FBL controller involving high-order derivative terms is presented, and then an adaptive SMC scheme is demonstrated using input augmentation in order to account for the underactuated nature of the quadrotor. Zuo (2010) introduces a new command-filtered BS control scheme based on the relationship between the attitude and linear acceleration of the quadrotor. In that method, the BS control scheme stabilizes the attitude subsystem and the linear tracking differentiator is employed for altitude stabilization. The proposed control scheme is designed as an alternative method for the classical inner/outer loop structure. Das et al. (2009) address an effective dynamic inversion method that can easily cope with the highly coupled nature of the quadrotor dynamics. Contrary
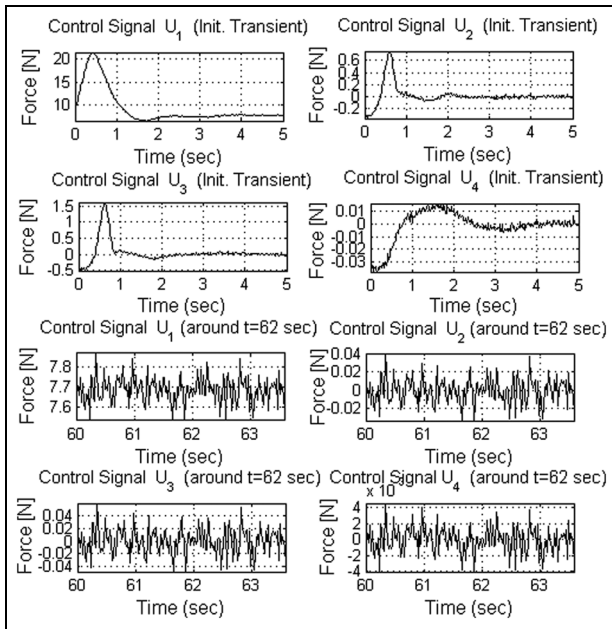
Figure 6. The control signals for the proportional-integral-derivative scheme for Set-1.

to classical dynamic inversion, the controller parameters can be designed uniquely to improve the tracking performance. Park et al. (2015) highlight a landing site search algorithm by using a vision system, which is used to obtain the depth map information of the terrain and flatness information of the topography. In that study, a controller is designed based on FBL and the linear quadratic tracker. The control strategy is assessed in terms of energy consumption, the flatness and the depth.

On the other hand, Cabecinhas et al. (2010) proposes non-linear controllers based on nested saturations for the tracking of arbitrary trajectories. A further FBL controller is developed by Mellinger and Kumar (2011) to obtain a desired thrust vector to track a minimum snap position trajectory. The desired thrust vector is used to generate a reference roll and pitch trajectory, which is followed by using a proportional plus derivative-type attitude controller. Fritsch et al. (2012) propose an exact input–output linearization controller for a nonlinear quadrotor model without uncertainties or exogenous disturbances. Ryan and Kim (2013) present a method for using linear matrix inequalities (LMIs) to synthesize controller gains for a quadrotor system. In that study, the controller is based on approximate FBL and is structured to allow PID tuning. A new nonlinear controller using a BS-like FBL method to control the quadrotor is addressed by Choi and Ahn (2014). The designed controller is divided into three sub-controllers, which are called the attitude controller, altitude controller and position controller. In addition, Kushleyev et al. (2012) design a micro quadrotor with onboard attitude estimation and control that operates autonomously with an external localization approach. Stability and parameter tuning methods of a double integral observer-based control scheme are addressed by Wang et al. (2015). A

novel state feedback controller is developed based on a quaternion representation of a model subject to uncertainties and external disturbances (Liu et al. 2015).

In the dynamic model of the quadrotor, the relative degrees and orders of the roll, pitch and yaw subsystems are the same. Input to state FBL can be applied to these three subsystems. The closed-loop system is reduced to three double integrators after applying inputs U_2, U_3, U_4, as formulated in (33)–(35):

$$U_2 = \frac{1}{p_3}(-p_1 x_4 x_6 - p_2 x_4 \Omega_r + v_1) \quad (33)$$

$$U_3 = \frac{1}{p_6}(-p_4 x_2 x_6 + p_5 x_2 \Omega_r + v_2) \quad (34)$$

$$U_4 = \frac{1}{p_6}(-p_5 x_2 x_6 + v_3) \quad (35)$$

Three double integrators are $\ddot{\phi} = v_1$, $\ddot{\theta} = v_2$, $\ddot{\psi} = v_3$. The signals denoted by v_i are selected as given in (36)–(38), where λ_1, $\lambda_2,\dots \lambda_6$ are design parameters and $s^2 + \lambda_1 s + \lambda_2 = 0$, $s^2 + \lambda_3 s + \lambda_4 = 0$ and $s^2 + \lambda_5 s + \lambda_6 = 0$ are Hurwitz:

$$v_1 = \ddot{\phi}_d + \lambda_1 \dot{e}_\phi + \lambda_2 e_\phi \quad (36)$$

$$v_2 = \ddot{\theta}_d + \lambda_3 \dot{e}_\theta + \lambda_4 e_\theta \quad (37)$$

$$v_3 = \ddot{\psi}_d + \lambda_5 \dot{e}_\psi + \lambda_6 e_\psi \quad (38)$$

Error signals are defined as $e_\phi = \phi_d - \phi$, $e_\theta = \theta_d - \theta$, $e_\psi = \psi_d - \psi$ and, with these choices, the tracking errors are governed by the following differential equations:

$$\ddot{e}_\phi + \lambda_1 \dot{e}_\phi + \lambda_2 e_\phi = 0 \quad (39)$$

$$\ddot{e}_\theta + \lambda_3 \dot{e}_\theta + \lambda_4 e_\theta = 0 \quad (40)$$

$$\ddot{e}_\psi + \lambda_5 \dot{e}_\psi + \lambda_6 e_\psi = 0 \quad (41)$$

Since the error dynamics of the vehicle attitude are stable, the desired attitude trajectories are to be followed.

Investigating the effects of the feedback linearization control parameters on control performance and design specifications. Since the technique removes the nonlinearities and shapes the error dynamics, we chose to observe the critically damped response in all three directions. For this purpose, user-defined parameters are chosen as given in Table 4, where different convergence speeds are enforced.

In Figure 7, the trajectory followed in the three-dimensional (3D) space is shown. Errors in the Cartesian space are depicted in Figure 8, where it is seen that the errors are acceptably small. Figure 9 illustrates the time evolution of the Euler angles; the produced control signals are shown in Figure 10. The figures show that the tracking precision is satisfactory under the presence of the measurement noise and the nested underactuated nature of the whole system

As mentioned previously, the ISCI index is the performance measure of the control input that is mainly affected by the high-magnitude control signals. Considering the three

controller sets, ISCI of Set-1 is the most appropriate one for practising the approach. Furthermore, as can be seen from Table 5, the MAE values are increasing when smaller controller parameters are taken into account. In addition, the ITSE and ISE parameters of Set-1 are better than those of Set-2 and Set-3. Therefore, in simulations producing Figures 7–10, coefficients of Set-1 are utilized.

Finally, it is worth mentioning that the FBL strategy has generated the maximum ISCI index compared to the other strategies, as seen in Table 6. This is particularly important when choosing the actuation hardware, which will be costly in this case.
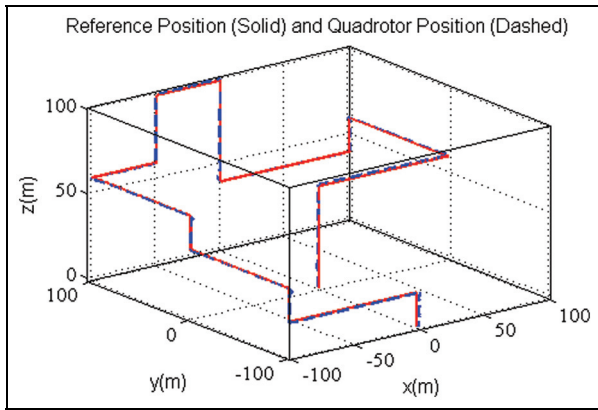

Figure 7. Tracking results for the feedback linearization control technique for Set-1.

A case study: backstepping control for the quadrotor. The BS method proposes an easy-to-use strategy to design a control loop for nonlinear systems (Bouabdallah and Siegwart, 2005; Castillo et al., 2006; Madani and Benallegue, 2007; Önkol and Efe, 2009). The design philosophy is based on the use of each state variable to stabilize the others through the state space model, organized in a chain structure from the input of the system to the output. Thus, the stabilization of every state variable is ensured individually. The controller design procedure of the BS method aims at constructing a recursive algorithm defining virtual states to make the control law computable. In order to use BS control effectively, the distinctive properties and the fundamental differences must be well defined. BS control is a powerful Lyapunov-based strategy for the stabilization of the nonlinear system that can be presented in nested loops (Krstic et al., 1995); the main advantage of BS control is the recursive use of Lyapunov function candidates. In addition, unlike FBL control with problems such as the precise model requirement and the cancellation of useful nonlinear terms, the BS approach offers a choice of design tools of nonlinearities. On the other hand, to guarantee the negativeness of the derivative of the Lyapunov function candidate, it usually requires the cancellation of some cross-coupling terms, which is the most prominent difference between BS control and SMC. Furthermore, the aforementioned cancellation may cause some performance degradation in terms of robustness. The major disadvantages of the BS approach are the difficulty in finding an appropriate Lyapunov function candidate for the system, sensitivity to parameter change and the necessity of full-state measurement.

The studies devoted to the BS control of the quadrotor can be summarized as follows: Bouabdallah and Siegwart

Table 4. The studied coefficients of the feedback linearizing controller.

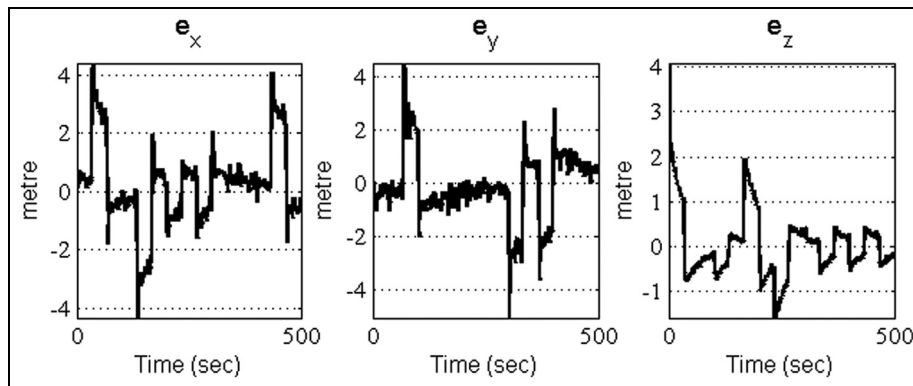|	λ_1	λ_2	λ_3	λ_4	λ_5	λ_6
Set-1	$2\sqrt{\lambda_2}$	12	$2\sqrt{\lambda_4}$	12	$2\sqrt{\lambda_6}$	12
Set-2	$2\sqrt{\lambda_2}$	6	$2\sqrt{\lambda_4}$	6	$2\sqrt{\lambda_6}$	6
Set-3	$2\sqrt{\lambda_2}$	3	$2\sqrt{\lambda_4}$	3	$2\sqrt{\lambda_6}$	3

Figure 8. Feedback linearization control results for the Cartesian space variables for Set-1.
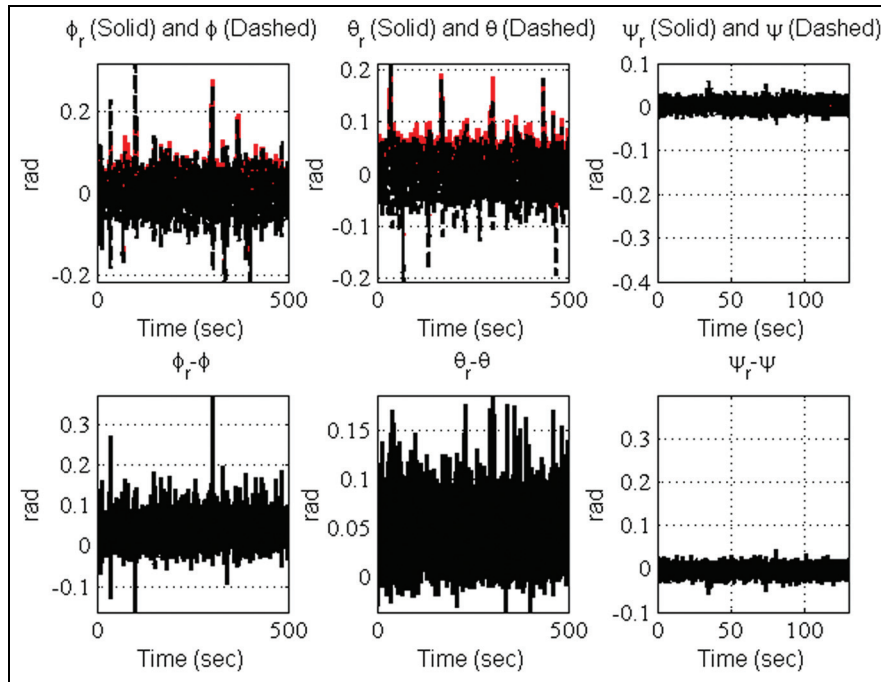
Figure 9. Results for the Euler angles (attitude) for Set-1.

Table 5. Measured performances of the feedback linearizing controller for three different parameter sets.

	Set-1			Set-2			Set-3		
	Pitch	Roll	Yaw	Pitch	Roll	Yaw	Pitch	Roll	Yaw
IAE	23.7081	22.2769	4.7256	30.75	26.155	6.6904	42.4042	34.888	12.489
MAE	0.1866	0.3708	0.0583	0.2723	0.3516	0.0817	0.4124	0.4959	0.1289
ISE	1.467	1.5576	0.0705	2.53	2.2512	0.1365	5.2538	4.2651	0.4454
ITSE	375.8	388.82	17.82	637.3029	541.6092	33.9564	1.3196	999.9845	111.336
EV	7.1595e-04	0.0014	1.1758e-04	0.0013	0.0028	1.5133e-04	0.0035	0.0071	3.4357e-04

IAE: integral absolute error; MAE: maximum absolute error; ISE: integral squared error; ITSE: integral time squared error; EV: error variance.

Table 6. Measured integral squared control input (ISCI) and control signal variances of the feedback linearizing controller for three different parameter sets.

Criterion	Control input	Set-1	Set-2	Set-3
ISCI	U_1	4.6474 e + 04	4.6572 e + 04	4.7247 e + 04
	U_2	513.9530	551.6272	618.3654
	U_3	197.7108	194.7696	229.3134
	U_4	0.0350	0.0161	0.0129
Control input variance	U_1	0.1423	0.1521	0.1945
	U_2	1.0269	1.1030	1.2367
	U_3	0.3941	0.3890	0.4584
	U_4	6.5172e-05	2.5879e-05	1.8473e-05

(2005) propose BS and SMC strategies to control both translational and angular dynamics of the quadrotor. Madani and Benallegue (2006) propose a full-state BS approach based on Lyapunov stability theory to follow the desired Cartesian trajectories. A further BS-based tracking control algorithm addresses the modified dynamical model, which contains a new expression of gyroscopic torque (Hamel and Mahony, 2007). However, the necessity of full-state information is a
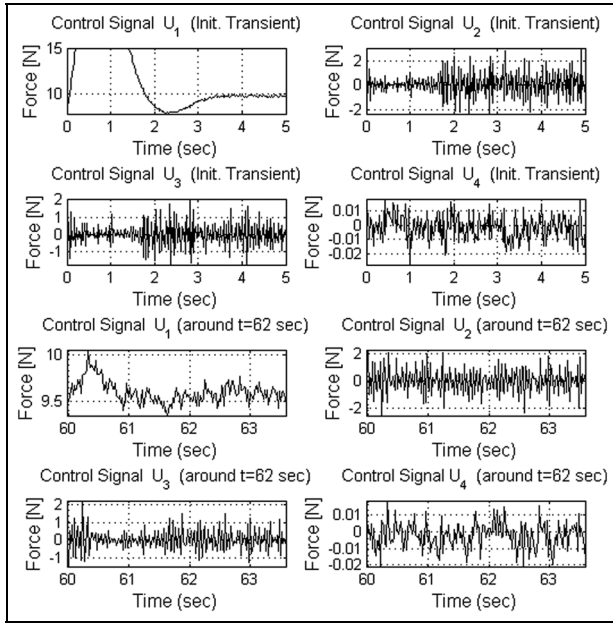
Figure 10. The control signals for the feedback linearization scheme for Set-1.

major drawback of these controllers. Guenard et al. (2008) present a visual servo control scheme by employing the BS approach with saturation functions that are employed for obtaining desired control signals. Another BS control scheme is introduced by Castillo et al. (2006), in which the controller is designed with a saturation function and it performs satisfactorily in the presence of perturbations. Furthermore, a modified BS approach, which decreases the number of the control parameters by half compared to the traditional BS approach used in the literature, is developed and applied to control the quadrotor UAV in Saif et al. (2012). In a recent study, Basri et al. (2015) proposed an intelligent BS controller based on the radial basis function neural network (RBFNN) as perturbation approximators. In that study, BS controller parameters are optimized based on the particle swarm optimization algorithm. On the other hand, a modified BS control strategy is employed in a 3D constrained tracking control algorithm (Ghommam et al., 2015). In another work, Ha et al. (2014) present a novel passivity-based adaptive BS control of underactuated quadrotors, using a stable haptic teleoperation application over the internet.

Remembering the model in (24)–(26), in order to design the BS controller, the first step is to define the virtual state and calculate the derivative of the virtual state as $v_1 := x_1 - x_{1d}$ and $v_2 := x_2 - \alpha_1 - \dot{x}_{1d}$, respectively. Choosing $V_1 = v_1^2/2$ as the Lyapunov function candidate for the first stage, the time derivative of V_1 is obtained as $\dot{V}_1 = v_1(v_2 + \alpha_1)$. If $\alpha_1 := -k_1 v_1$ is selected, then $\dot{V}_1 = -k_1 v_1^2 + v_1 v_2$ is obtained. For the second stage, the Lyapunov function candidate $V_2 = V_1 + v_2^2/2$ is chosen. Since

$$\dot{v}_2 = p_1 x_4 x_6 + p_2 x_4 \Omega_d + p_3 U_2 - (-k_1 \dot{v}_1) - \ddot{x}_{1d} \quad (42)$$

the time derivative of V_2 can be written as below:

$$\dot{V}_2 = \dot{V}_1 + v_2 \dot{v}_2 = -k_1 v_1^2 \\ + v_2(p_1 x_4 x_6 + p_2 x_4 \Omega_d + p_3 U_2 - (-k_1 \dot{v}_1) - \ddot{x}_{1d}) \quad (43)$$

with $k_2 > 0$; if the control law is as given in (44), then the time derivative of V_2 can be written as in (45):

$$U_2 = \frac{1}{p_3}(-v_1 - p_1 x_4 x_6 - p_2 x_4 \Omega_d - k_1(z_2 - k_1 v_1) + \ddot{x}_{1d} - k_2 v_2)$$
$$(44)$$

and

$$\dot{V}_2 = -k_1 v_1^2 - k_2 v_2^2 \quad (45)$$

Repeating the same procedure for the pitch and yaw dynamics, one obtains U_3 and U_4 as follows:

$$U_3 = \frac{1}{p_6}(-v_3 - p_4 x_2 x_6 + p_5 x_2 \Omega_d - k_3(v_4 - kv_3) + \ddot{x}_{3d} - k_4 v_4)$$
$$(46)$$

$$U_4 = \frac{1}{p_8}(-v_5 - p_7 x_2 x_4 - k_5(v_6 - k_5 v_5) - k_6 v_6) \quad (47)$$

These control signals ensure the Lyapunov stability of the closed-loop system.

Investigating the effects of backstepping control parameters on control performance and design specifications. A number of simulation studies are carried out in MATLAB/Simulink® to find the most convenient parameters to drive the states of the quadrotor satisfying the desired values. Noisy observations are considered to analyse the disturbance rejection capability of the closed-loop control system and different sets of parameters are chosen and their effects on the performance are assessed.

Three sets of parameters are studied and the values chosen are tabulated in Table 7. In order to observe faster convergence in the positional variables, relevant coefficients are chosen larger than those influencing the velocities. The obtained performance values are summarized in Table 8. The comparison of the ISCI and control signal variances for the BS controller is presented in Table 9.

The quality of the closed-loop system's response and control signal are quantified by ISE, IAE and ISCI performance indices. The main goal of the BS control approach is to eliminate the large errors and fluctuations in a reasonable time range, so that the ISE converges to a relatively small value. Variations of the error signals are kept under a predefined acceptable range of ISE and IAE indices. However, the cross-coupling cancellation of the BS strategy may cause relatively large magnitude control signals and potentially poor robustness against uncertainties. In Table 7, Set-3 displays most appropriate performance indices compared to other sets applied.

The controller performance index ISCI exhibits the magnitude of the control signal. Considering the three controller sets, the ISCI of the first set is the most appropriate one for

Table 7. The studied coefficients of the backstepping controller.

	k_1	k_2	k_3	k_4	k_5	k_6
Set-1	1	0.5	1	0.5	1	0.5
Set-2	2	1	2	1	2	1
Set-3	10	5	10	5	10	5

Table 8. Measured performances of the backstepping controller for three different parameter sets.

Criterion	Set-1			Set-2			Set-3		
	Pitch	Roll	Yaw	Pitch	Roll	Yaw	Pitch	Roll	Yaw
IAE	9.0398	2.4625	1.6722	6.6738	1.8560	1.3957	3.6150	2.5912	1.3180
MAE	0.0842	0.0468	0.0427	0.0543	0.0368	0.0240	0.0452	0.0440	0.0159
ISE	0.2027	0.0256	0.0108	0.1086	0.0125	0.0064	0.0387	0.0216	0.0055
ITSE	50.9746	6.3957	2.2792	27.189	3.0258	1.5177	9.5160	5.1204	1.3579
EV	9.8336e-05	4.2604e-05	1.8920e-05	4.6502e-05	1.7616e-05	1.2344e-05	3.1448e-05	2.2142e-05	1.0967e-05

IAE: integral absolute error; MAE: maximum absolute error; ISE: integral squared error; ITSE: integral time squared error; EV: error variance.

Table 9. Measured integral squared control input (ISCI) and control signal variances of the backstepping controller for three different parameter sets.

Criterion	Control input	Set-1	Set-2	Set-3
ISCI	U_1	9.80900e + 04	9.80930 e + 04	9.89710 e + 04
	U_2	28.7015	29.1660	32.8089
	U_3	21.4519	22.5848	30.4720
	U_4	0.97380	0.30520	0.04020
Control input variance	U_1	0.7710	0.7703	0.7658
	U_2	0.0574	0.0583	0.0654
	U_3	0.0429	0.0452	0.0605
	U_4	1.8633e-07	6.0447e-07	8.0319e-05

Table 10. Simulation parameters for the sliding mode control scheme.

Simulation time	T	500 s
Simulation step size	Δt	0.02 s
Slope parameters	$\lambda_\varphi, \lambda_\theta, \lambda_\Psi$	1.00
Angular measurement noise variance	$\Delta\phi, \Delta\theta, \Delta\Psi$	1e−5 rad
Sign function smoothing parameter	ε	0.10
Initial values of Euler angles	$\phi(t_0), \theta(t_0), \psi(t_0)$	0.3 rad

Figure 11. The tracking results for the backstepping control technique for Set-1.

real-time applications. ISCI values of the BS controller are quite large with respect to the PID alternative. The reason for observing large yet quickly converging errors is the aggressively stabilizing nature of the chosen nonlinear control approach. A closer look at the result in Tables 7–9 indicates that the performance of the BS controller is influenced from changes in the controller parameters and the performance deterioration occurs when the parameters decrease. The simulation parameters are described in Table 10. The demonstrated BS control strategy satisfactorily enforces the quadrotor to desired altitude and attitude position, as shown in Figures 11–14.
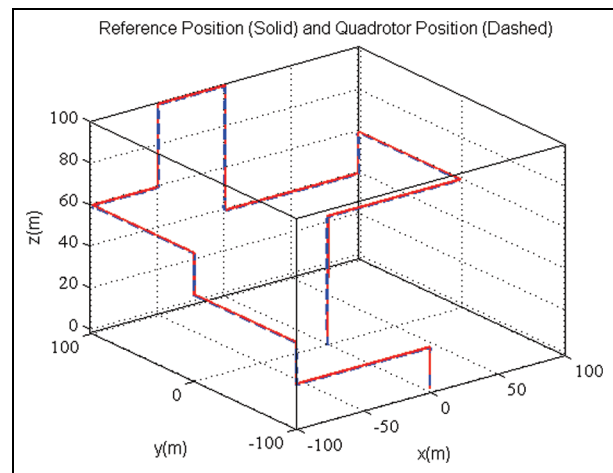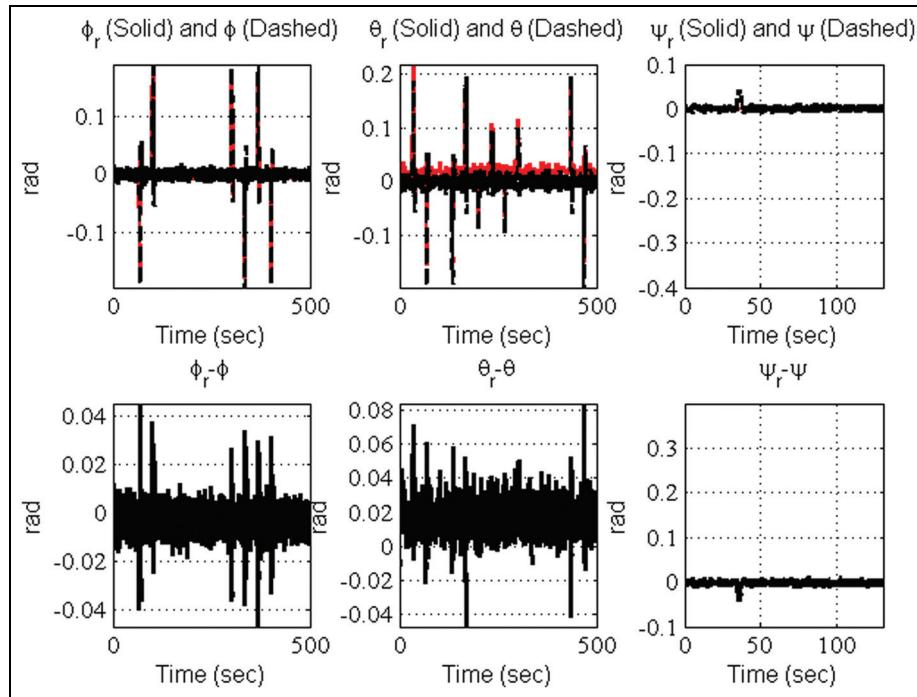
Figure 12. Results for the Euler angles (attitude) for Set-1.
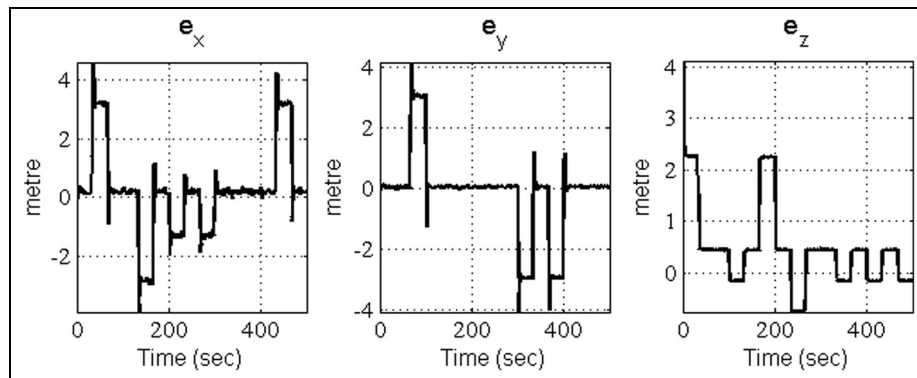

Figure 13. Backstepping control results for the Cartesian space variables for Set-1.

A case study: sliding mode controller design for the quadrotor. SMC is a popular robust control technique displaying a number of prominent features, such as robustness, accuracy and easy parameter tuning. Thus, the SMC strategy can be applied to a wide range of nonlinear systems encountered in various application areas, such as robotics, mechatronics and the automotive industry.

In SMC, the response in the phase space is guided towards a predefined subspace of the state space called the switching subspace, which is the sole attractor of the phase plane. The switching subspace is stable and the trajectories trapped to it converge to the origin. The latter dynamic regime is called the sliding mode and the control technique borrows its name from this particular regime (Efe, 2011a; Khalil, 1996; Slotine and Li, 1991). The main philosophy of the SMC approach is the

design of a switching hypersurface in the phase space spanned by the error and its derivatives, such that the selected subspace is stable and its attractor is at the origin.

Numerous works have been reported on SMC of the quadrotor. Bouabdallah and Siegwart (2005), for instance, address SMC application on the OS4 platform. Madani and Benallegue (2007) highlight a sliding mode controller driven by a sliding mode disturbance observer (SMC-SMDO) approach to estimate the translational and angular velocities of the quadrotor. A discontinuous SMC obtaining asymptotic regulation of a quadrotor to the origin with a desired yaw angle and known model parameters is presented by Xu and Özgüner (2006). Efe (2007) elaborate a SMC scheme to obtain a robust control of the quadrotor aerial robot; hence, this leads to robustness against disturbances and modelling
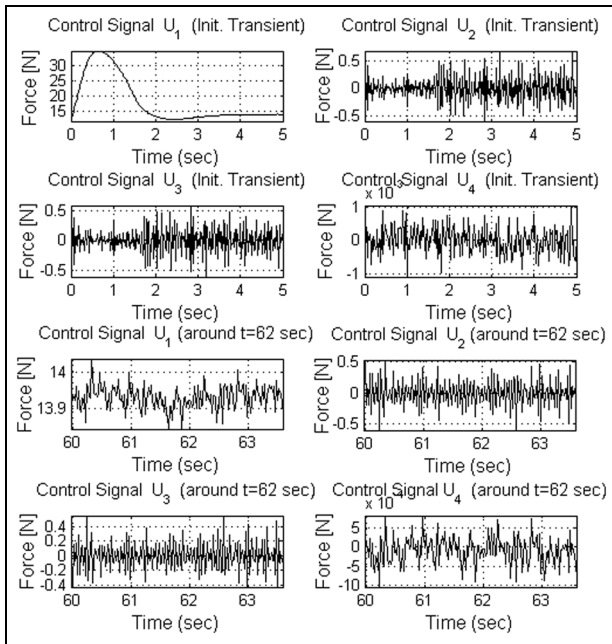
Figure 14. The control signals for the backstepping scheme for Set-1.

errors, which are encountered frequently in the low-level control of actuation mechanism of UAVs. In addition, Gonzalez et al. (2013) present the real-time implementation of the theoretical results given by Efe (2007). Benallegue et al. (2008) present a higher order SMC scheme that is combined with a robust differentiator. However, this approach still has some detrimental effects on the transient response of the system, which is critically important for high manoeuvre capability. Thus, in order to cope with such disadvantages, a block control technique combined with the second-order SMC scheme based on the use of the super-twisting algorithm is proposed for designing a flight controller, which is capable of tracking the desired Cartesian trajectory (Derafa et al., 2012). This strategy achieved finite-time convergence, but it requires precise knowledge of the inertia matrix. A trajectory tracking performance is elaborated by Chen et al. (2015) for a quadrotor subject to unknown parameters. The proposed solution contains sliding mode observers for fault-tolerant control. In that study, in order to ensure the robustness, an online adaptive estimation is proposed to learn the parameter changes. Bouchoucha et al. (2011) present a robust second-order SMC for the attitude stabilization of a quadrotor subject to external bounded disturbances. Efe (2011a) propose an integral SMC with fractional order reaching dynamics. Sanchez et al. (2012) propose a second-order SMC to achieve exponential tracking of the quadrotor attitude with a semi-global uniformly ultimately bounded position tracking. Meguenni et al. (2012) demonstrate a fuzzy integral sliding mode-BS method for an X4-flyer type quadrotor. In that method, the integral action is supported by a fuzzy inference system to eliminate the static error. Moreover, a saturation function was considered as a boundary layer to reduce the chattering phenomenon. Besnard et al. (2012) present the recently developed the SMC-SMDO approach to design a robust flight control

scheme for a quadrotor where the proposed control scheme does not use the high gain property of the SMC. Zheng et al. (2014) highlight a second-order SMC in order to get rid of the undesired chattering phenomenon. In that study, the nonlinear coefficients of the defined switching sliding manifold are investigated via the Hurwitz technique. Xiong and Zheng (2014) present a further controller synthesis scheme to generate high-performance position and attitude tracking control. In that study, a novel robust terminal SMC algorithm is proposed and a second-order SMC scheme is employed to reduce the effect of the chattering phenomenon.

The design in this paper is only demonstrated for the roll axis, but the same approach can be repeated for the other axes. As a first step of the implementation, define $e_\phi := \phi - \phi_d$ as the error in roll dynamics and chose the switching variable as $s_\phi = \dot{e}_\phi + \lambda_\phi e_\phi$. The sliding subspace (surface) is designed according to the relative degree between the output and the input of the system. When $s_\phi = 0$ is reached at time t_0, the solution after t_0 is obtained as $e_\phi(t) = e_\phi(t_0) \exp(-\lambda_\phi(t - t_0))$. Now consider the Lyapunov function candidate as

$$V(s_\phi) = \frac{1}{2} s_\phi^2 \qquad (48)$$

If the time derivative of the Lyapunov function candidate satisfies $s_\phi \dot{s}_\phi < -k_\phi |s_\phi|$ with $k_\phi > 0$, then all initial conditions of the roll error are guided towards the loci characterized by $s_\phi = 0$. To maintain $s_\phi \dot{s}_\phi < -k_\phi |s_\phi|$, the control signal is chosen as follows:

$$U_2 = \frac{1}{p_3} \left(-p_1 x_4 x_6 - p_2 x_4 \Omega_d + \ddot{x}_{1d} - \lambda_\phi(x_2 - \dot{x}_{1d}) - k_\phi sign(s_\phi) - k_1 s_\phi \right) \qquad (49)$$

where $\dot{x}_{1d}$ is the desired angular roll rate and $\ddot{x}_{1d}$ the desired angular roll acceleration. In order to avoid chattering during the implementation stage, the sign function is approximated as $sign(x) \cong x/(|x| + \varepsilon)$ with a parameter, ε, determining the sharpness around $s_\phi = 0$. The approach is repeated for U_3 and U_4, and the following discontinuous feedback control laws are obtained:

$$U_3 = \frac{1}{p_6} \left(-p_4 x_2 x_6 + p_5 x_2 \Omega_d + \ddot{x}_{3d} - \lambda_\theta(x_4 - \dot{x}_{3d}) - k_\theta sign(s_\theta) - k_2 s_\theta \right) \qquad (50)$$

$$U_4 = \frac{1}{p_8} \left(-p_7 x_2 x_4 + \ddot{x}_{5d} - \lambda_\psi(x_6 - \dot{x}_{5d}) - k_\psi sign(s_\psi) - k_3 s_\psi \right) \qquad (51)$$

The original forms of the control laws above provide the highest level of robustness, yet the control signal is very much vulnerable to noise available in the measurements. The smaller values of ε provide better tracking performance yet larger values provide better control signal characteristics. The balance between the two conflicting design specifications is established after a study of parameter refinement.

Table 11. The studied coefficients of the sliding mode control scheme.

	λ_φ	λ_θ	λ_Ψ	k_φ	k_θ	k_Ψ	k_1	k_2	k_3
Set-1	1	1	1	0.5	0.5	0.5	0.5	0.5	0.5
Set-2	1	1	1	1	1	1	1	1	1
Set-3	3	2	3	5	5	5	5	5	5

Table 12. Measured performances of the sliding mode control scheme for three different parameter sets.

Criterion	Set-1			Set-2			Set-3		
	Pitch	Roll	Yaw	Pitch	Roll	Yaw	Pitch	Roll	Yaw
IAE	6.9269	4.0910	1.3161	5.7036	3.9268	1.3006	5.8262	5.3163	1.3044
MAE	0.0593	0.0753	0.0159	0.0487	0.0607	0.0161	0.0567	0.0445	0.0154
ISE	0.1262	0.0571	0.0055	0.0839	0.0464	0.0053	0.0856	0.0772	0.0054
ITSE	31.8131	14.0241	1.3608	21.3849	11.9611	1.3299	22.0331	20.0368	1.3367
EV	6.7076e-05	7.2059e-05	1.0880e-05	4.1683e-05	3.9532e-05	1.0645e-05	4.1552e-05	4.6130e-05	1.0716e-05

IAE: integral absolute error; MAE: maximum absolute error; ISE: integral squared error; ITSE: integral time squared error; EV: error variance.

Table 13. Measured integral squared control input (ISCI) and control signal variances of the sliding mode controller for three different parameter sets.

Criterion	Control input	Set-1	Set-2	Set-3
ISCI	U_1	4.3523 e + 04	4.3590 e + 04	4.5957e + 04
	U_2	63.9705	66.9137	107.5510
	U_3	152.3928	56.4994	93.2395
	U_4	0.0012	0.0046	0.2386
Control input variance	U_1	0.1722	0.1724	0.1990
	U_2	0.1279	0.1338	0.2146
	U_3	0.1048	0.1130	0.1859
	U_4	2.3321e-06	9.2889e-06	4.7714e-04

Investigating the effects of the SMC parameters on control performance and design specifications. Choosing different parameter sets leads to different performance figures. The increase in the gain of the sign function makes the switching subspace a stronger attractor and the robustness of the closed-loop system increases. The price paid for this is the vulnerability of the closed loop to noises that provoke the chattering phenomenon. For a better reaching phase response when the error vector is away from the switching subspace, the reaching law can be augmented by other terms. The other fundamental parameter is λ_i, which defines the unique pole of the reduced dynamics of the system. The considered coefficient sets are described in Table 11, where parameters with different magnitudes are focussed on. In Tables 12 and 13, the results obtained with the SMC technique are presented and the behaviour observed in 3D space is illustrated in Figure 15. The followed path is close to the reference and the time domain results with the presented flight are depicted in Figures 16–19.
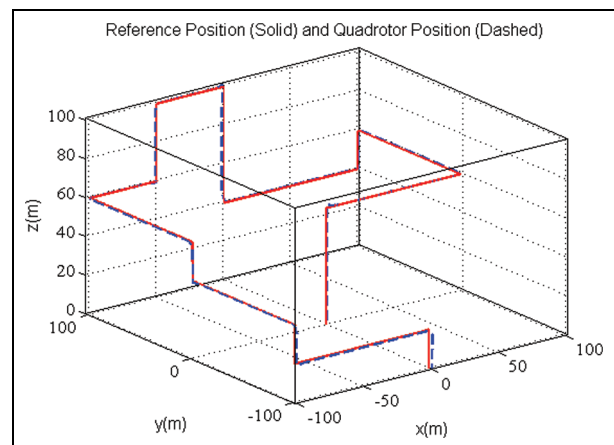
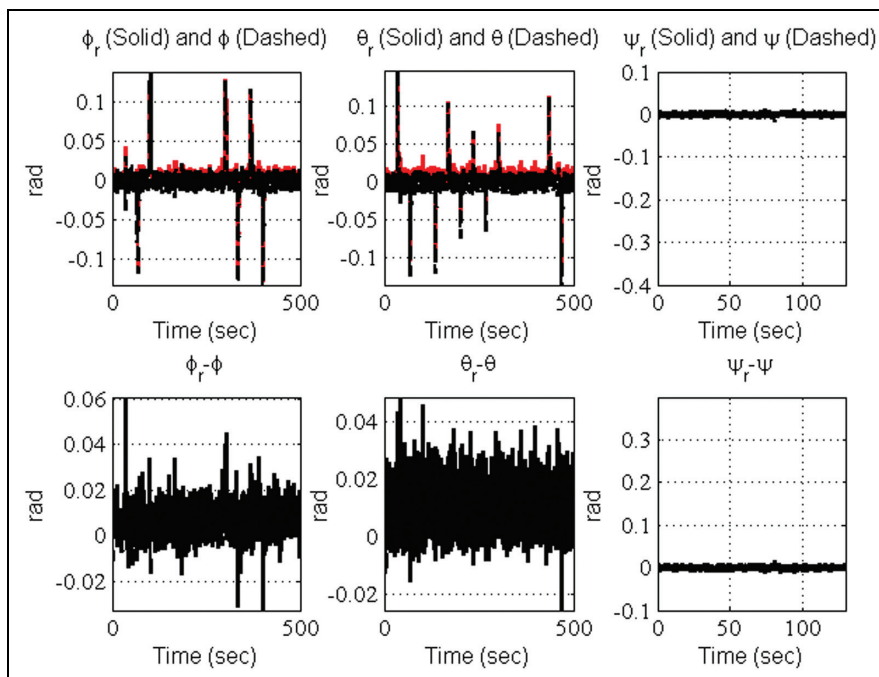**Figure 15.** The tracking results for the sliding mode control technique for Set-2.

Figure 16. Results for the Euler angles (attitude) for Set-2.
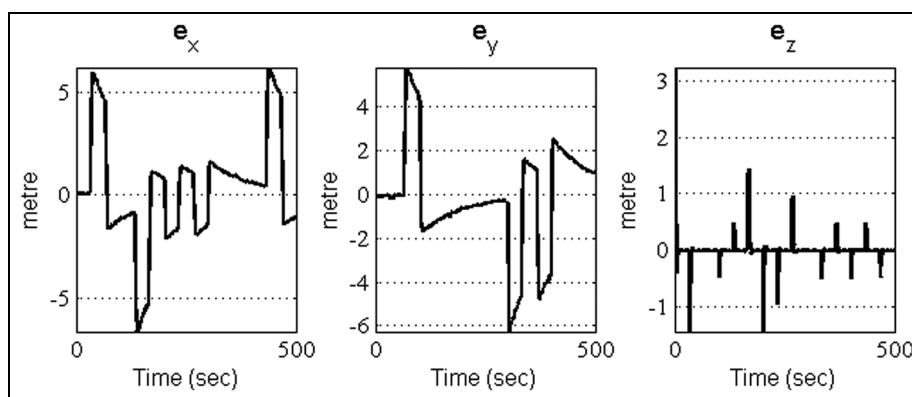

Figure 17. Sliding mode control results for the Cartesian space variables for Set-2.

In particular, the results seen in Figure 18 justify the emergence of the sliding regime and the stable maintenance of it.

During the selection of the controller parameters, the real system's behaviour is taken into consideration in order to avoid claiming physically impossible manoeuvres. This is particularly important as the control signals should be kept within certain limits. The real time experimentation would have a similar nature when refining the controller parameters. According to the ISCI index, Set-2 is the most appropriate one for prototyping the system in real time. Furthermore, ITSE and ISE measurements of Set-2 are better than those of Set-1 and Set-3. This observation leads us to recommend the coefficients of Set-2.

The major advantage of the SMC is its robustness against uncertainties in the system dynamics and the disturbances caused by different sorts of internal and external factors. This is a substantial advantage in UAV control applications. Simplicity and low computational burden are commonly accepted advantages of the SMC technique. However, it is still necessary to elucidate further issues, before all the benefits of SMC can be harvested. The chattering phenomenon, arising from fast switching conditions and consisting of fast variations in the control signal, is the most prevalent handicap of the SMC technique. In this study, a continuous approximation of the sign function is employed for eliminating the chattering phenomenon. However, the price paid for this is a boundary layer around the switching subspace. A number of algorithms, such as higher order sliding mode and the super-twisting algorithm, have been proposed to minimize the chattering phenomenon. Indeed, to remedy the detrimental effect of the chattering, several works have proposed a combination of SMC with fuzzy logic control.
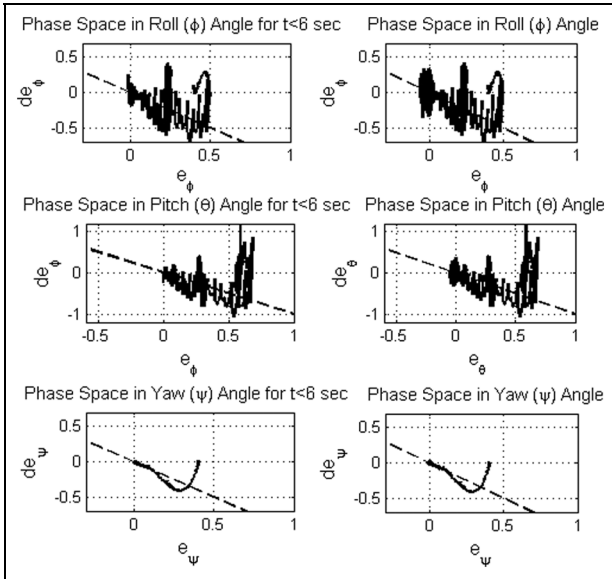
Figure 18. Phase space behaviour for Set-2.
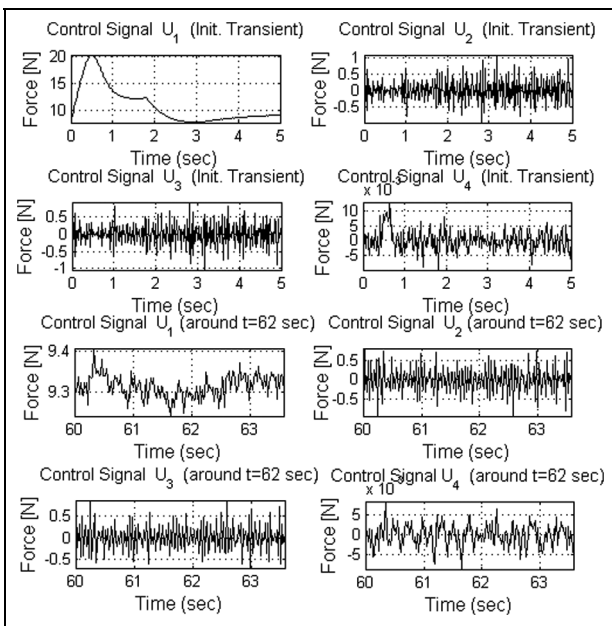

Figure 19. The control signals for the sliding mode control scheme for Set-2.

As seen in Figure 18, the error vector for each Euler angle converges to the corresponding sliding subspace. Furthermore, s_ϕ and s_ψ converge faster than s_θ, which is a desired result observed with parameter Set-3. The performance of the SMC is satisfactory except for the variation in process gain, where it takes a considerable amount of time to settle.

Adaptive and learning based control strategies. Adaptive control strategies are efficient methods for aerial robots because

of their capability of alleviating unmodelled dynamics and unstructured atmospheric disturbances (Dydek, 2010; Roberts and Tayebi, 2011). There have been a great number of studies devoted to adaptive control of quadrotor-type UAVs. Sadeghzadeh et al. (2011) propose an adaptive control scheme based on the Massachusetts Institute of Technology (MIT) rule to provide robustness against sensor and actuator faults. In another work, Dydek et al. (2013) address a model reference adaptive control (MRAC) scheme based on Lyapunov stability theory. The proposed control scheme combines the direct and indirect adaptation in order to enhance the tracking performance and parameter estimation accuracy. Nicol et al. (2011) present a direct approximate-adaptive controller, which is designed by nonlinear approximators employing Cerebellar Model Articulation Controller (CMAC), for an experimental application on a prototype quadrotor aerial robot. Mellinger and Kumar (2011) highlight a machine learning approach to perform acrobatic manoeuvres. An adaptive fuzzy controller is designed to stabilize the quadrotor in the presence of sinusoidal wind disturbance. In order to stabilize the quadrotor in the presence of this type of a disturbance, an alternative membership function (MF) is proposed for the adaptation process (Coza et al., 2011). This controller can handle sinusoidal-type disturbances. Dierks and Jagannathan (2009) present an adaptive neural network controller that stabilized the quadrotor in a simulation environment. A novel robust adaptive tracking algorithm based on a Lyapunov-like energy function is presented for a quadrotor subject to modelling error and disturbance uncertainties (Park et al., 2015). Moreover, Efe (2011b) proposed a neural network assisted computationally simple $PI^\lambda D^\mu$ controller demonstrating the use of fractional order control schemes. Alexis et al. (2011, 2012) propose a switching-based model predictive control (MPC) scheme for attitude control of a quadrotor subject to an atmospheric disturbances scenario.

The switching procedure is designed by the rate of the rotation angles. In a more recent study, Cabecinhas et al. (2014) demonstrate a nonlinear adaptive state feedback tracking controller for a quadrotor. They achieved asymptotical stability in the presence of force disturbances. In this method, angular actuation divided into two methods: angular velocity and torque. The actuation does not grow unbounded as a function of the position error. Lee (2013) proposed a robust adaptive tracking control system for the attitude dynamics of a quadrotor. The suggested control scheme can asymptotically follow an attitude trajectory without the knowledge of the inertia matrix, and it is expanded to guarantee the boundedness of the attitude tracking errors in the case of non-parametric disturbances. Chen et al. (2014) highlight an adaptive compensation control method that is derived via a disturbance observer (DO) and quantum information processing approach. Although the system has unknown partial actuator failures and external disturbances, the proposed scheme can overcome the attitude tracking problem effectively.

A case study: fuzzy logic control design for UAV control. The fuzzy logic control strategy has been employed to solve various control problems due to its suitability to describe the control laws in terms of verbal expressions. The approach is rule

based and it interpolates the local verbal descriptions to obtain the desired global controller. The intuitive design, in which the designer does not need a precise model, is the major advantage of the fuzzy logic control. In Özbek and Efe (2010), the fuzzy controller is developed based on the expert knowledge and past experiences of the designer. The controller does not need the information about plant parameters or a detailed mathematical model (Syed and Gueaib, 2010). The fuzzy controllers are designed in the light of the knowledge acquired through an expert's observations about the system. Technically speaking, the fuzzy logic-based controller is a nonlinear controller and its local behaviour can be adjusted through the rules defining the local functions. Although the fuzzy logic strategy can be employed for the control of complex nonlinear dynamical systems, it may be tedious to prove stability and robustness rigorously. Under some assumptions, adaptive fuzzy systems display very good performance with analytically proven stability. Erginer and Altuğ (2012) present the design and implementation of a hybrid fuzzy logic control scheme for a quadrotor. Rabhi et al. (2011) design a Takagi–Sugeno (T-S) fuzzy controller to obtain the desired closed-loop control performance. The proposed controller is developed by using LMIs. Another learning-based fuzzy control scheme is proposed by Liu et al. (2014). In that study, a novel learning-based LQR technique is developed by employing an extended Kalman filter (EKF), which is used to optimize the Mamdani fuzzy controller by adjusting the shapes of the MFs. Ilhan and Karaköse (2013) design a type-2 fuzzy controller for the quadrotor UAV. Bhantkhande and Havens (2014) address a real-time intelligent neuro-fuzzy control scheme, where a classical PD controller is employed to train an Adaptive Neuro Fuzzy Inference System (ANFIS). Furthermore, the feasibility of the developed control strategy in a model-in-the-loop simulation is demonstrated. A networked fuzzy controller and H_∞ feedback control scheme is presented by Han et al. (2014). The nonlinear model of the quadrotor is approximated by a T-S fuzzy model and the network-induced delays and packet dropouts are modelled in a unified framework.

Returning the attitude stabilization of a quadrotor UAV in hand, a fuzzy system with 49 rules is utilized. The fuzzy controller for each Euler angle is implemented separately. The rules have been formed by using triangular MFs and with a product inference engine. The output MFs are singletons and the overall input–output relation is given as below:

$$u = \frac{\sum\limits_{i=1}^{R} y_i \prod\limits_{j=1}^{m} \mu_{ij}(e_j)}{\sum\limits_{i=1}^{R} \prod\limits_{j=1}^{m} \mu_{ij}(e_j)} \qquad (52)$$

where $\mu_{ij}(e_j)$ is the MF quantifying the ith rule's jth input, which is e_j. The rule structure of the fuzzy logic controller is summarized as below. In this rule base, NB, NM, NS, Z, PS, PM, PB denote the labels negative big, negative medium, negative small, zero, positive small, positive medium, positive big, respectively:
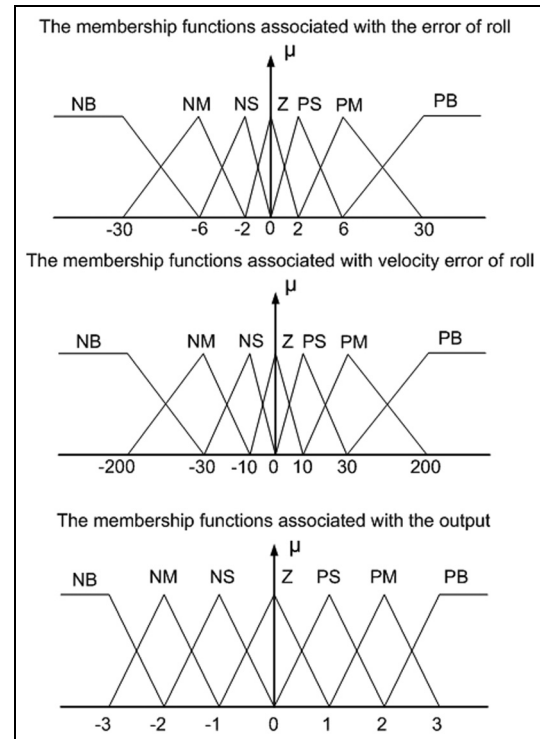

Figure 20. Structure of the membership functions for the fuzzy controller (membership functions Set-1).

$$\mathbf{IF}(e_1 \text{ is NB}) \text{ AND } (\dot{e}_1 \text{ is NB})\mathbf{THEN}(u = y_1)$$
$$\vdots$$
$$\mathbf{IF}(e_1 \text{ is PB}) \text{ AND } (\dot{e}_1 \text{ is PB})\mathbf{THEN}(u = y_{49})$$

In the implementation stage, triangular MFs are used as illustrated in Figure 20. The obtained controller is constructed for each axis and the measurements for the fuzzy controllers are read as degrees. The defuzzifier parameters, denoted by y_i, are chosen between –3 and 3, which is determined according to the observations from the already studied control schemes. The weighted average defuzzification technique is employed for obtaining the crisp output. The rule table of the proposed fuzzy control scheme is given in Table 14. The results obtained with the fuzzy controller are given in Figure 21, where it is seen that the attitude stabilization is obtained with a very good level of precision. The control surface formed by the fuzzy controller is depicted in Figure 22, where it can be seen that the fuzzy control mechanism provides a soft interpolation between the local decisions prescribed by the rule base. The produced control signal is shown in Figure 23, and the performance indicators are tabulated in Tables 15 and 16. The fuzzy control scheme is seen as the best performing approach in terms of ISE measure.

Since the SAA is one underlying assumption in the design, another fuzzy controller design is made considering the MFs associated with the error from the interval (–10,10) degrees and the MFs associated with the rate of error from the interval (–40,40) degrees/s. The defuzzifier parameters are chosen between (–1.5,1.5) in the new fuzzy scheme and called Set-2 in

Table 14. Fuzzy rules.

$\dot{e}$ \ e	NB	NM	NS	Z	PS	PM	PB
NB	NB	NB	NM	NM	NS	NS	Z
NM	NB	NM	NM	NS	NS	Z	PS
NS	NM	NM	NS	NS	Z	PS	PS
Z	NM	NS	NS	Z	PS	PS	PM
PS	NS	NS	Z	PS	PS	PM	PM
PM	NS	Z	PS	PS	PM	PM	PB
PB	Z	PS	PS	PM	PM	PB	PB
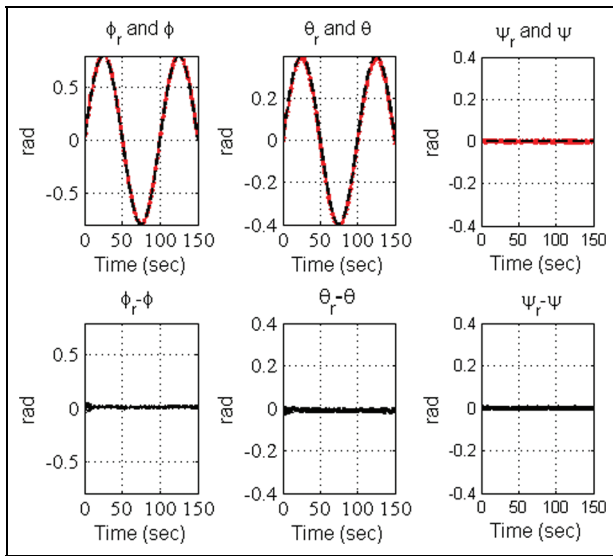
Figure 21. Results for the Euler angles (attitude).

Figure 22. Fuzzy surface.

Figure 23. The control signals for the fuzzy logic control scheme for membership functions.

performs better and the results associated with the first experiment are given in the subsequent figures.

Discussion on the performance of the control strategies

This study presents a performance assessment and a comprehensive survey of representative control schemes used for designing autopilots for quadrotor UAVs. The elaborated control strategies are being studied actively to cope with nonlinear and coupled dynamics, aerodynamic effects, actuator faults, saturations, perturbations and modelling uncertainties. The chosen performance metrics are EV, IAE, MAE, ITSE and ISE. The radar charts of the comparisons are shown in Figures 24 and 25. Since the criteria are different and they yield values that are away from others, different scale factors have been chosen to attain the same levels of magnitude,

Tables 15 and 16. The tracking performance of the fuzzy controller is presented in Table 15 and the produced control signal is given in Table 16. It is shown in these tables that Set-1
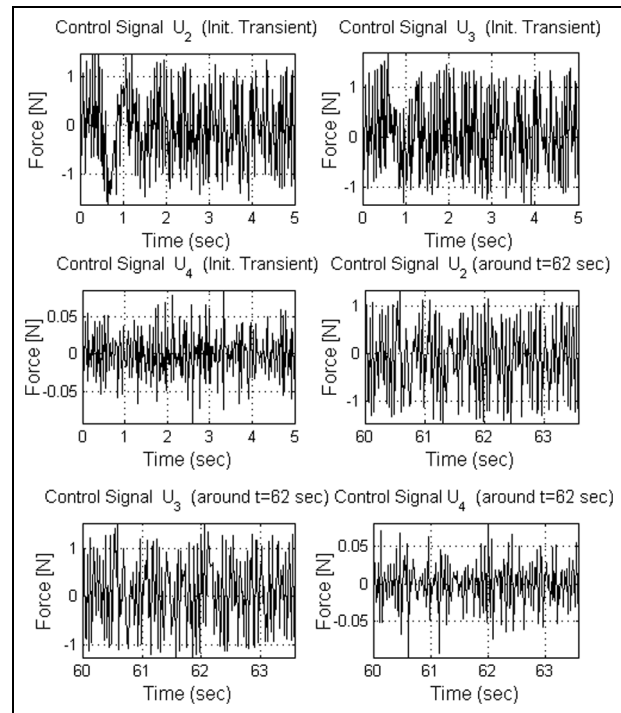
Table 15. Measured performances of the fuzzy logic controller for two different membership function sets.

	Membership function Set-1			Membership function Set-2		
	Pitch	Roll	Yaw	Pitch	Roll	Yaw
IAE	3.6845	3.7080	1.4562	9.8652	9.7881	1.5443
MAE	0.0650	0.0419	0.0155	0.0985	0.0714	0.0249
ISE	0.0443	0.0457	0.0075	0.3136	0.3104	0.0097
ITSE	10.9548	11.1771	1.9040	54.8799	53.6075	2.1113
EV	3.1132e-05	3.2045e-05	1.1938e-05	3.7940e-05	3.8039e-05	1.3335e-05

IAE: integral absolute error; MAE: maximum absolute error; ISE: integral squared error; ITSE: integral time squared error; EV: error variance.
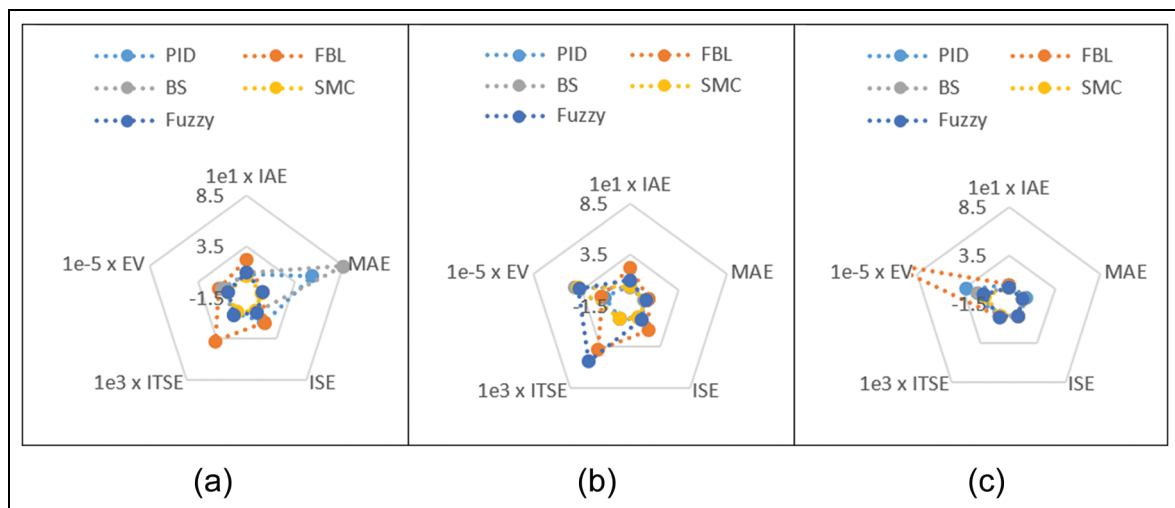

Figure 24. Performance results of the control strategies for the angular dynamics: (a) roll dynamics; (b) pitch dynamics; (c) yaw dynamics.

Table 16. Measured integral squared control input (ISCI) and control signal variances of the fuzzy logic controller for two different membership function sets.

Criterion	Control input	Set-1	Set-2
ISCI	U_2	330.5792	206.3989
	U_3	330.3649	206.5827
	U_4	0.5026	1.5854
Control input variance	U_2	0.6509	0.3979
	U_3	0.6513	0.3981
	U_4	0.0010	0.0032

thereby showing a proper visualization of the differences between the methods.

The comparison of the control performance of rotational dynamics, based on radar diagrams, is presented in Figure 24. According to the figure, SMC and the BS controller achieve the most accurate control; however, the magnitude of the control signal of BS control is relatively larger than SMC. Furthermore, the results show that the convergence during the transient phase is faster with the BS than that with the FBL technique. The control signal obtained via FBL is simpler; thus, it is convenient for practical applications. However, in terms of the EV, the poorest results were obtained with the FBL controller, which fails in producing a smooth control signal.

Furthermore, in order to qualify the overall performance of the control strategies, some statistical analysis methods, such as the sum of the ISE, the sum of the MAE, actuation step, computational complexity and control energy consumption, are chosen as metrics for the comparison.

1. The sum of the ISE in Cartesian coordinates $\int_t e_x^2 dt + \int_t e_y^2 dt + \int_t e_z^2 dt$.
2. The sum of the ISE with rotational dynamics: $\int_t e_\phi^2 dt + \int_t e_\theta^2 dt + \int_t e_\psi^2 dt$.
3. The sum of the MAE in Cartesian coordinates: $\max|e_x| + \max|e_y| + \max|e_z|$.
4. The sum of the MAE with rotational dynamics: $\max|e_\phi| + \max|e_\theta| + \max|e_\psi|$.
5. The number of actuation steps.
6. The computational complexity.
7. The energy consumption. The sum of the four rotors; squared angular speeds: $\sum_1^4 \int_t \omega_i^2 dt$.
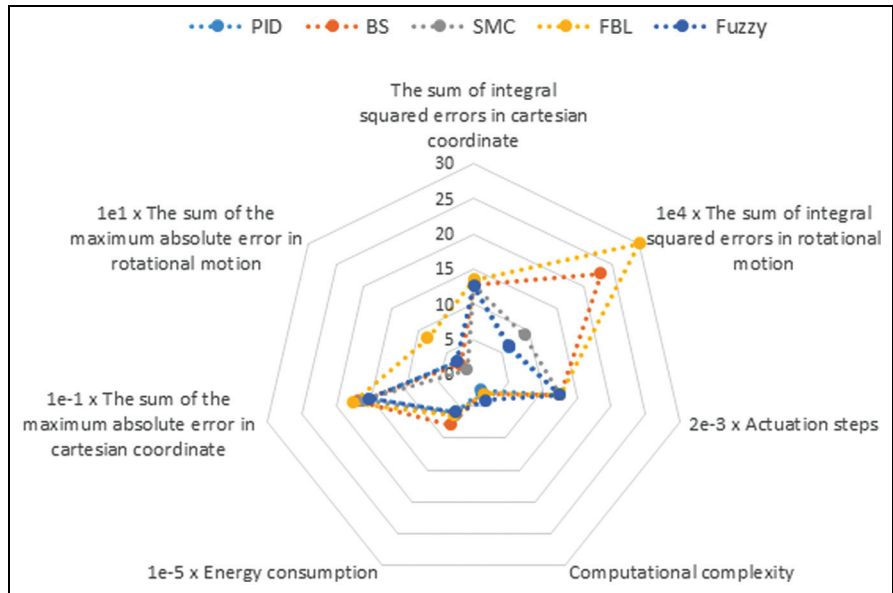
Figure 25. The comparison of the control strategies with respect to the above performance metrics.

Table 17. Advantages and drawbacks of dedicated control strategies for unmanned aerial vehicle research.

Control Strategy	Advantages	Drawbacks	Improvements
PID Scheme	• Less energy consumption • Low computation cost	• Poor performance if the linearized system behaviour is dissimilar to true system • Lack of robustness • Limited operated range	• Parameter optimization and automatic tuning can be adapted • Event-triggered and resource aware controller can be proposed • Intelligent techniques can be combined
Feedback linearization	• Smooth control signal	• Cannot cope with model parameter changes • Needs an exact model • Larger error variance • High sensitivity to parameter changes	• Strong robustness and adaptability can be provided • Event-triggered and resource aware controller can be designed
Backstepping control	• Robust • Fast response	• Large magnitude control signals • Possible cancellation during the controller design • Necessity to the full-state measurement	• Strong robustness and adaptability can be provided • Reduce control effort can be proposed
Sliding mode control	• Robust • Simple structure • Easy parameter tuning	• Chattering • Considerable energy consumption	• Chattering can be eliminated • Adaptability can be provided
Intelligent and adaptive control strategies: fuzzy logic control	• Model-free design • Use of expert knowledge • Wide operation range • Nonlinearities can be eliminated or reduced	• Analytical stability proof is missing • Needs an expert for a good initialization • Lack of robustness	• Robustness can be provided with Type II fuzzy approaches • Optimal controller can be designed

PID: proportional-integral-derivative.

In terms of the controller structure, the PID scheme is easy to implement and it performs better when the exact knowledge about the system dynamics are used to determine the controller parameters. However, it should be noted that, in any practical application, some part of the system is known very poorly (e.g. friction, turbulence, etc.). Thus, successful flight under the presence of disturbances and modelling errors becomes a challenge for approaches that entail precise plant models. This study considers such difficulties to display the performance of every scheme, and to give an idea about their real-time implementation costs.

In terms of the response time, the BS control scheme outperforms its alternatives. This is an important criterion, as the changes in air conditions are rapid and a control system is desired to respond quickly.

According to the results obtained, PID control without disturbance has the smallest tracking error, yet the performance decreases significantly under the presence of disturbances and uncertainties. As the information about the plant under control becomes descriptive, one can utilize nonlinear control schemes to obtain a better performance.

From the application point of view, the SMC scheme, despite its simplicity, provides a strong robustness against a wide class of uncertainties. The design process in SMC considers the physical variables, while that in the BS approach considers intermediate variables. Both result in a stable closed loop, yet the SMC scheme directly manipulates the physical variables, that is, the errors, and therefore the comprehensibility of SMC is higher than that of the BS approach.

Regarding the computational complexity, undoubtedly the PID scheme is the simplest. A balance, seeking a good closed-loop performance and simplicity, places the SMC scheme among the methods considered. The algorithmic simplicity of SMC makes it realizable on low-cost microprocessor platforms with very good tracking performance and robustness against disturbances and uncertainties. The sole input to the design procedure is the nominal system model, which fits the quadrotor problem in hand.

Contributions and conclusions

This paper presents the application of PID, BS, SMC, FBL and fuzzy control techniques on a quadrotor-type UAV, which is a frequently used as a test bed for a number of research studies. The methods have been assessed with a number of comparison metrics and several parameter sets have been chosen for each approach. The results illustrate the different aspects of the chosen control strategies and the observations are tabulated in the paper.

The contributions of this paper are as follows: (i) describing a sample set of feedback control experiments for the quadrotor-type aerial robot to strengthen the notion of linear and nonlinear control with a complete literature survey; (ii) providing researchers with an overview of linear, nonlinear and adaptive control algorithms developed for stabilization and trajectory tracking applications of the quadrotor aerial robot; (iii) describing a set of performance criteria for a frequently utilized aerial robot; (iv) determining the best

Table 18. Best performing approach.

Metric	Best performing approach
IAE	Sliding mode control (Set-2)
MAE	Sliding mode control (Set-2)
ISE	Fuzzy logic control (Set-1)
ITSE	Backstepping control (Set-3)
EV	Backstepping control (Set-3)
ISCI	PID (Set-1)
Control input variance	PID (Set-1)
Tracking precision	Sliding mode control (Set-2)
Energy consumption	PID (Set-1)

IAE: integral absolute error; MAE: maximum absolute error; ISE: integral squared error; ITSE: integral time squared error; EV: error variance; ISCI: integral squared control input; PID: proportional-integral-derivative.

performing scheme according to control effort and tracking precision metrics.

Table 17 presents advantages and drawbacks of dedicated control strategies for unmanned aerial vehicle research. Table 18 summarizes the results of this paper. According to the table, for a quadrotor UAV, the best tradeoff between tracking precision and control accuracy is observed with the SMC approach.

References

Alexis K, Nikolakopoulos G and Tzes A (2011) Switching model predictive attitude control for a quadrotor helicopter subject to atmospheric disturbances. *Control Engineering Practice* 19: 1195–1207.

Alexis K, Nikolakopoulos G and Tzes A (2012) Model predictive quadrotor control: attitude, altitude and position experimental studies. *Control Theory & Applications, IET* 6: 1812–1827.

Altuǧ E, Ostrowski JP and Taylor CJ (2003) Quadrotor control using dual camera visual feedback. In: *proceedings of the IEEE international conference on robotics and automation*, pp. 4294–4299.

Araar O and Aouf N (2014) Full linear control of quadrotor UAV: LQ and H∞. In: *proceedings of the UKACC international conference on control*, pp.133–138.

Basri MAM, Husain AR and Kumerasan AD (2015) Intelligent adaptive backstepping control for MIMO uncertain non-linear quadrotor helicopter systems. *Transactions of the Institute of Measurement and Control* 37: 345–361.

Belkheiri M, Rabhi A, Hajjaji AE, et al. (2012) Different linearisation control techniques for a quadrotor system. In: *proceedings of the 2nd international conference on communications, computing and control applications (CCCA)*, pp.1–6.

Benallegue A, Mokhtari A and Fridman L (2008) High-order sliding-mode observer for a quadrotor UAV. *International Journal of Robust and Nonlinear Control* 18: 427–440.

Bergamasco M and Lovera M (2014) Identification of linear models for the dynamics of a hovering quadrotor. *IEEE Transactions on Control System Technology* 22: 1696–1707.

Besnard L, Shtessel Y, Landrum B, et al. (2012) Quadrotor vehicle control via sliding mode controller driven by sliding mode disturbance observer. *Journal of the Franklin Institute* 349: 658–684.

Bhantkhande P and Havens TC (2014) Real time fuzzy controller for quadrotor stability control. *Proceedings of the IEEE International Conference on Fuzzy Systems (FUZZ-IEEE)*, pp.913–919.

Bouabdallah S (2007) *Design and control of quadrotors with application to autonomous flying*. PhD Thesis, Ecole Polytechnique Fédérale de Lausanne, Switzerland.

Bouabdallah S, Murrieri P and Siegwart R (2004a) Design and control of an indoor micro quadrotor. In: *proceedings of the IEEE international conference on robotics and automation*, pp.4393–4398.

Bouabdallah S, Noth A and Siegwart R (2004b) PID vs LQ control techniques applied to an indoor micro quadrotor. In: *proceedings of the IEEE/RSJ international conference on intelligent robots and systems (IROS 2004)*, pp.2451–2456.

Bouabdallah S and Siegwart R (2005) Backstepping and sliding-mode techniques applied to an indoor micro quadrotor. In: *proceedings of the 2005 IEEE international conference on robotics and automation*, pp.2247–2252.

Bouabdallah S and Siegwart R (2007) Full control of a quadrotor. In: *proceedings of the IEEE/RSJ international conference on intelligent robots and systems*, pp.153–158.

Bouchoucha M, Seghour S and Tadjine M (2011) Classical and second order sliding mode control solution to an attitude stabilization of a four rotors helicopter: from theory to experiment. In: *proceedings of the IEEE international conference on mechatronics (ICM 2011)*, pp.162–169.

Cabecinhas D, Cunha R and Silvestre C (2014) A nonlinear quadrotor trajectory tracking controller with disturbance rejection. *Control Engineering Practice* 26: 1–10.

Cabecinhas D, Naldi R, Marconi L, et al. (2010) Robust take-off and landing for a quadrotor vehicle. In: *proceedings of the IEEE international conference on robotics and automation*, pp.1630–1635.

Cai G, Dias J and Seneviratne L (2014) A survey of small-scale unmanned aerial vehicles: recent advances and future development trends. *Unmanned System* 2: 175–199.

Carrillo LRG, Dzul A and Lozano R (2012) Hovering quadrotor control: A comparison of nonlinear controllers using visual feedback. *IEEE Transactions on Aerospace and Electronic Systems* 48: 3159–3170.

Castillo P (2004) *Modelling and control of a helicopter with four rotors*. PhD Thesis, HeuDiaSyc, UTC, Compiegne, France.

Castillo P, Albertos P, Garcia P, et al. (2006) Simple real-time attitude stabilization of a quad-rotor aircraft with bounded signals. In: *proceedings of the 45th IEEE conference on decision and control*, pp.1533–1538.

Castillo P, Dzul A and Lozano R (2004) Real-time stabilization and tracking of a four-rotor mini rotorcraft. *IEEE Transactions on Control Systems Technology* 12: 510–516.

Castillo P, Lozano R and Dzul EA (2005) *Modelling and Control of Mini-Flying Machines*. New York: Springer, pp.317–322.

Chen F, Lu F, Jiang B, et al. (2014) Adaptive compensation control of the quadrotor helicopter using quantum information technology and disturbance observer. *Journal of the Franklin Institute* 351(1): 442–455.

Chen F, Zhang K, Wang Z, et al. (2015) Trajectory tracking of a quadrotor with unknown parameters and its fault-tolerant control via sliding mode fault observer. *Journal of Systems and Control Engineering* 229: 279–292.

Choi Y-C and Ahn H-S (2014) Nonlinear control of quadrotor for point tracking: Actual implementation and experimental test. *IEEE/ASME Transactions on Mechatronics* 20(3): 1179–1192.

Cowling ID, Yakimenko OA, Whidborne J F, et al. (2007) A prototype of an autonomous controller for a quadrotor UAV. In: *proceedings of the European control conference*, pp.532–536.

Coza C, Nicol C, Macnab JBC, et al. (2011) Adaptive fuzzy control for a quadrotor helicopter robust to wind buffeting. *Journal of Intelligent & Fuzzy Systems: Applications in Engineering and Technology* 22: 267–283.

Das A, Subbarao K and Lewis F (2009) Dynamic inversion with zero-dynamics stabilization for quadrotor control. *IET Control Theory and Applications* 3: 303–314.

Derafa L, Benallegue A and Fridman L (2012) Super-twisting control algorithm for the attitude tracking of a four-rotors UAVs. *Journal of Franklin Institute* 349: 685–699.

Dierks T and Jagannathan S. (2009) Output feedback control of a quadrotor UAV using neural networks. *IEEE Transactions on Neural Networks* 21: 50–66.

Driessen S and Pounds PIE (2013) Towards a more efficient quadrotor configuration. In: *proceedings of the IEEE/RSJ international conference on intelligent robots and systems*, pp.1386–1392.

Dydek ZT (2010) *Adaptive control of unmanned aerial systems*. PhD Thesis, Department of Mechanical Engineering, Massachusetts Institute Technology, Cambridge, USA.

Dydek ZT, Annaswamy AM and Lavretsky E (2013) Adaptive control of quadrotor UAVs: A design trade study with flight evaluations. *IEEE Transactions on Control System Technology* 21: 1400–1407.

Efe MÖ (2007) Robust low altitude behavior control of a quadrotor rotorcraft through sliding modes. In: *proceedings of the Mediterranean conference on control and automation*, pp.1–6.

Efe MÖ (2011a) Integral sliding mode control of a quadrotor with fractional order reaching dynamics. *Transactions of the Institute of Measurement and Control* 33: 985–1003.

Efe MÖ (2011b) Neural network assisted computationally simple PI-lambda D-mu control of a quadrotor UAV. *IEEE Transactions on Industrial Informatics* 7: 354–361.

Elsamanty M, Khalifa A, Fanni M, et al. (2013) Methodology for identifying quadrotor parameters, attitude estimation and control. In: *proceedings of the IEEE/ASME international conference on advance mechatronics*, pp.1343–1348.

Erginer B and Altuğ E (2007) Modeling and PD control of a quadrotor VTOL vehicle. In: *proceedings of the IEEE intelligent vehicles symposium*, pp.894–899.

Erginer B and Altuğ E (2012) Design and implementation of a hybrid fuzzy logic controller for a quadrotor VTOL vehicle. *International Journal of Control, Automation and Systems* 10: 61–70.

Fritsch O, Monte PD, Buhl M, et al. (2012) Quasi-static feedback linearisation for the translational dynamics of a quadrotor helicopter. In: *proceedings of the American control conference (ACC)*, pp.125–130.

Gee SS, Lee TH and Tan EG (1998) Adaptive neural network control of flexible joint robots based on feedback linearisation. *International Journal of Systems Science* 29: 623–635.

Ghommam J, Charland G and Saad M (2015) Three-dimensional constrained tracking control via exact differentiation estimator of a quadrotor helicopter. *Asian Journal of Control* 17: 1093:1103.

Gonzalez I, Salazar S, Lozano R, et al. (2013) Real-time altitude robust controller for a quadrotor aircraft using sliding mode control techniques. In: *proceedings of the international conference on unmanned aircraft systems*, pp.650–659.

Gremillion G (2010) System identification of a quadrotor micro air vehicle. In: *proceedings of the AIAA atmospheric flight mechanics conference, AIAA-2010–7644*, Toronto, Canada.

Guenard N, Hamel T and Mahony R (2008) A practical visual servo control for unmanned aerial vehicle. *IEEE Transactions on Robotics* 24: 331–340.

Guerrero-Castellanos JF, Téllez-Guzman JJ, Durand S, et al. (2013) Event-triggered nonlinear control for attitude stabilization of a quadrotor. In: *proceedings of the international conference on unmanned aircraft systems (ICUAS)*, pp.84–591.

Gupte S, Hohandas PIT and Conrad JM (2012) A survey of quadrotor aerial vehicles. In: *proceedings of IEEE Southeastcon*, pp.978–983.

Gurdan D, Stumpf J, Achtelik M, et al. (2007) Energy-efficient autonomous four-rotor flying robot controlled at 1 kHz. In: *proceedings of the IEEE international conference on robotics and automation*, pp.361–366.

Ha CJ, Zuo CS, Choi FB, et al. (2014) Passivity-based adaptive backstepping control of quadrotor-type UAVs, *Robotics and Autonomous Systems* 62: 1305–1315.

Hamel T and Mahony R (2007) Image based visual servo-control for a class of aerial robotic systems. *Automatica* 43: 1975–1983.

Hamel T, Mahony R, Lozano R, et al. (2002) Dynamic modelling and configuration stabilization for an X4-flyer. In: *proceedings of the IFAC world congress*, pp.200–212.

Han F, Feng G, Wang Y, et al. (2014) Fuzzy modeling and control for a nonlinear quadrotor under network environment. In: *proceedings of the IEEE international conference on cyber technology, automation, control and intelligent systems (CYBER)*, pp.395–400.

Hoffer NV, Coopmans C, Jensen AM, et al. (2014) A survey and categorization of small low-cost unmanned aerial vehicle system identification. *Journal of Intelligent and Robotic Systems* 74: 129–145.

Hoffmann G, Huang H, Waslander SL, et al. (2011) Precision flight control for a multi vehicle quadrotor helicopter test bed. *Control Engineering Practice* 19: 1023–1036.

Hoffmann G, Rajnarayan DG, Waslander SL, et al. (2004) The Stanford testbed of autonomous rotorcraft for multi-agent control (STARMAC). In: *23rd digital avionics system conference*, pp.121–130.

Hua M-D, Hamel T, Morin P, et al. (2009) A control approach for thrust-propelled underactuated vehicles and its application to VTOL drones. *IEEE Transactions on Automatic Control* 54: 1837–1853.

Hua M-D, Hamel T, Morin P, et al. (2013) Introduction to feedback control of underactuated VTOL vehicles. *IEEE Control Systems Magazine* 33(1): 61–75.

Ilhan I and Karaköse M (2013) Type-2 fuzzy based quadrotor control approach. *Proceedings of the Asian Control Conference (ASCC)*, pp.1–6.

Iskandarani M, Givigi SN, Rabbath CA, et al. (2013) Linear model predictive control for the encirclement of a target using a quadrotor aircraft. In: *proceedings of the 21st Mediterranean control and automation conference*, pp.1550–1556.

Islam S, Liu PX and Saddik AE (2015) Robust control of four-rotor unmanned aerial vehicle with disturbance uncertainty. *IEEE Transactions on Industrial Electronics* 62: 1563–1571.

Kalantari A and Spenko M (2015) Modeling and performance assessment of the HyTAQ, a hybrid terrestrial/aerial quadrotor. *IEEE Transactions on Robotics* 30: 1278–1285.

Khalil H (1996) *Nonlinear Systems*. Upper Saddle River, NJ: Prentice Hall, pp.519–570.

Kim JH, Kang M-S and Park S (2010) Accurate modelling and robust hovering control of quadrotor VTOL aircraft. *Journal of Intelligent and Robotic Systems* 57: 9–26.

Korpela CM, Danko TW and Oh PY (2012) MM-UAV: mobile manipulation unmanned aerial vehicle. *Journal of Intelligent and Robotics Systems* 65: 93–101.

Krstic M, Kanellakopoulos I and Kokotovic P (1995) *Nonlinear and Adaptive Control Design*. Third Avenue, New York, NY: John Wiley and Sons.

Kushleyev A, Mellinger D, Powers C, et al. (2012) Towards a swarm of agile micro quadrotors. *Autonomous Robots* 35: 287–300.

Lai L-V, Yang C-C and Wu C-J (2006) Time-optimal control of a hovering quadrotor helicopter. *Journal of Intelligent and Robotic Systems* 45: 115–135.

Lee D, Kim J and Sastry S (2009) Feedback linearisation vs adaptive sliding mode control for a quadrotor helicopter. *International Journal of Control, Automation and Systems* 7: 419–428.

Lee T (2013) Robust adaptive attitude tracking on SO(3) with an application to a quadrotor UAV. *IEEE Transactions on Control Systems Technology* 21: 1924–1930.

Li J and Li Y (2011) Dynamic analysis and PID control for a quadrotor. In: *proceedings of the IEEE international conference on mechatronics and automation*, pp.126–131.

Liu H, Wang X and Zhong Y (2015) Quaternion-based robust attitude control for uncertain robotic quadrotors. *IEEE Transactions on Industrial Informatics* 11: 406–415.

Liu ZX, Yuan C, Zhang YM, et al. (2014) A learning-based fuzzy LQR control scheme for height control of an unmanned quadrotor helicopter. In: *proceedings of the international conference on unmanned aircraft systems (ICUAS)*, pp.936–941.

Lozano R (2010) *Unmanned Air Vehicles: Embedded Control*. St George's Road, London: Wiley-ISTE.

Lugue-Vega L, Castillo-Toledo B and Loukianov A G (2012) Robust block second order control for a quadrotor. *Journal of Franklin Institute* 349: 719–739.

Lupashin S, Schoelling A, Shernack M, et al. (2010) A simple learning strategy for high-speed quadrotor multi-flips. *Proceedings of the IEEE International Conference Robotics and Automation*, pp.642–648.

Madani T and Benallegue A (2006) Control of a quadrotor Mini-Helicopter via full state backstepping technique. In: *proceedings of the 2006 IEEE conference on decision & control*, pp.1515–1520.

Madani T and Benallegue A (2007) Sliding mode observer and backstepping control for a quadrotor unmanned aerial vehicles. In: *proceedings of the 2007 American control conference*, pp.5887–5892.

Mahony R and Kumar V (2012) Special issue: Aerial robotics and the quadrotor platform. *IEEE Robotics & Automation Magazine* 19: 19.

Mahony R, Kumar V and Corke P (2012) Multirotor aerial vehicles: Modelling, estimation and control of quadrotor. *IEEE Robotics & Automation Magazine* 19: 20–32.

Meguenni KZ, Tahar M, Benhadria MR, et al. (2012) Fuzzy integral sliding mode based on backstepping control synthesis for an autonomous helicopter. *Proceedings of the Institution of Mechanical Engineers, Part G: Journal of Aerospace Engineering* 227: 751–765.

Meier L, Tanskanen P, Fraundorfer F, et al. (2011) PIXHAWK: a system for autonomous flight using onboard computer vision. In: *proceedings of the IEEE international conference on robotics and automation*, pp.2992–2997.

Mellinger D and Kumar V (2011) Minimum snap trajectory generation and control for quadrotors. In: *proceedings of the IEEE international conference on robotic and automation*, pp.2520–2525.

Mellinger D, Michael N and Kumar V (2014) Trajectory generation and control of precise aggressive maneuvers. *Springer Transactions in Advanced Robotics* 79: 361–373.

Mian AA and Daobo W (2008) Nonlinear flight control strategy for underactuated quadrotor aerial robot. In: *proceedings of the IEEE international conference on networking, sensing and control*, pp.938–942.

Mukherjee P and Waslander SL (2012) Direct adaptive feedback linearisation for quadrotor control. In: *AIAA guidance, navigation and control conference,* DOI: 10.2514/6.2012–4917.

Nicol C, Macnab CJB and Ramirez SA (2011) Robust adaptive control of a quadrotor helicopter. *Mechatronics* 21: 927–938.

Oner KT, Cetinsoy E, Unel M, et al. (2008) Dynamic model and control of a new quadrotor unmanned aerial vehicle with tilt-wing mechanism. In: *Proceedings of the World Academy Science Engineering and Technology*, pp. 58–63.

Önkol M and Efe M.Ö (2009) Experimental nonlinear control algorithms for a Quadrotor unmanned vehicle. In: *proceedings of the 2nd international symposium on unmanned vehicles*, pp.191–221.

Orsag M, Poropat M and Bogdan S (2010) Hybrid fly-by-wire quadrotor controller. In: *proceedings of the IEEE international symposium on industrial electronics*, pp.202–207.

Özbek NS and Efe MÖ (2010) Swing up and stabilization control experiments for rotary inverted pendulum-An educational comparison. In: *proceedings of the IEEE system man and cybernetic conferences*, pp.2226–2231.

Park J, Kim Y and Kim S (2015) Landing site searching and selection algorithm development using vision system and its application to quadrotor. *IEEE Transactions on Control System Technology* 20: 488–503.

Pounds P (2008) *Design, construction and control of a large quadrotor micro air vehicle*. PhD Thesis, Australian National University, Australia.

Rabhi A, Chadli M and Pegard C (2011) Robust fuzzy control for stabilization of a quadrotor. In: *proceedings of the international conference on advanced robotics (ICAR)*, pp.471–475.

Reyes-Valeria E, Enriquez-Caldera R, Camacho-Lara S, et al. (2013) LQR control for quadrotor using unit quaternions: Modelling and simulation. In: *proceedings of the international conference on electronics, communication and computing*, pp.172–178.

Roberts A and Tayebi A (2011) Adaptive position tracking of VTOL UAVs. *IEEE Transactions on Robotics* 27: 129–142.

Ryan T and Kim HJ (2013) LMI-based gain synthesis for simple robust quadrotor control. *IEEE Transactions on Automation Science and Engineering* 10: 1173–1178.

Ryll M, Bülthoff H and Giardano PR (2014) A novel overactuated quadrotor unmanned aerial vehicle: Modelling, control and experimental validation. In: *proceedings of the IEEE control system technology*, 10.1109/TCST.2014.2330999.

Sadeghzadeh I, Mehta A, Chamseddine A, et al. (2012) Active fault tolerant control of a quadrotor UAV based on gain scheduled PID control. In: *proceedings of the 25th IEEE Canadian conference on electrical & computer engineering (CCECE)*, pp.1–4.

Sadeghzadeh I, Mehta A and Zhang Y (2011) Fault/damage tolerant control of a quadrotor helicopter UAV using model reference adaptive control and gain-scheduled PID. In: *proceedings of the AIAA guidance, navigation, and control conference*, pp.1–10.

Saif A, Dhaifullah M, Al-Malki M, et al. (2012). Modified backstepping control of quadrotor. In: *proceedings of the 9th international multi-conference on systems, signals and devices (SSD)*, pp.1–6.

Samad T and Annaswamy AM (2011) The impact of control technology. Technical Report, IEEE Control Systems Society.

Sanchez A, Escareno J, Garcia O, et al. (2008) Autonomous hovering of noncyclic tilt-rotor UAV: Modelling, control and implementation. In: *proceedings of the IFAC world congress*, pp. 803–808.

Sanchez A, Parra-Vega V, Tang C, et al. (2012) Continuous reactive-based position-attitude control of quadrotors. In: *proceedings of the American control conference (ACC)*, pp.4643–4648.

Schoelling A, Augugliaro F, Lupashin S, et al. (2010) Synchronizing the motion of a quadrocopter to music. In: *proceedings of the IEEE international conference robotics and automation*, pp.3355–3360.

Seborg DE, Edgar TF and Mellichamp DA (1989) *Process Dynamics and Control.* New York: Wiley.

Senkul F and Altuğ E (May 2013) Modelling and control of a novel tilt: Roll rotor quadrotor UAV. In: *proceedings of the international conference on unmanned aircraft systems*, pp.1071–1076.

Slotine JJE and Li W (1991) *Applied Nonlinear Control.* Englewood Cliffs, New Jersey, NJ: Prentice Hall, pp. 207–271.

Syed RA and Gueaib W (2010) Intelligent flight control of an autonomous quadrotor. In: Casolo F (ed.) *Motion Control.* Vukovar, Croatia: InTech.

Tayebi A and McGilvray A (2006) Attitude stabilization of a VTOL Quadrotor Aircraft. *IEEE Transactions on Control Systems Technology* 14: 562–571.

Toledo J, Acosta L, Perea D, et al. (2015) Stability and performance analysis of unmanned aerial vehicles: Quadrotor against Hexrotor. *IET Control Theory Applications* 9: 1190–1196.

Toledo LAJ, Sigut M and Felipe J (2009) Stabilization and altitude tracking of four-rotor micro helicopter using lifting operators. *IET Control Theory and Application* 3: 452–464.

Tomic T, Schmid K, et al. (2012) Towards a fully autonomous UAV: Research platform for indoor and outdoor urban search and rescue. *IEEE Robotics & Automation Magazine* 19: 46–56.

Voos H (2009) Nonlinear control of quadrotor micro-UAV using feedback linearisation. In: *proceedings of the IEEE international conference on mechatronics*, pp. 1273–1278.

Wang J, Geamanu M-S, Cela A, et al. (2013) Event driven model free control of quadrotor. In: *proceedings of the IEEE international conference on control applications*, pp.722–727.

Wang J, Monuier H, Cela A, et al. (2011) Event driven intelligent PID controllers with applications to motion control. In: *proceedings of the 18th IFAC world congress (IFAC2011)*, pp. 10080–10085.

Wang X, Shirinzadeh B and Ang M H (2015) Nonlinear double-integral observer and application to quadrotor aircraft. *IEEE Transactions on Industrial Electronics* 62: 1189–1200.

Wu J, Peng H, Chen Q, et al. (2014) Modeling and control approach to a distinctive quadrotor helicopter. *ISA Transactions* 53: 173–185.

Xiong JJ and Zheng EH (2014) Position and attitude tracking control for a quadrotor UAV. *ISA Transactions* 53: 725–731

Xu R and ÖzgünerÜ (2006) Sliding mode control of a Quadrotor Helicopter. In: *proceedings of the 45th IEEE international conference on decision & control*, pp.4957–4962.

Zhang C, Li S and Ding S (2012) Finite-time output feedback stabilization and control for quadrotor mini-aircraft. *Kybernetika* 48: 206–222.

Zhang X, Li X, Wang K, et al. (2014) A survey of modelling and identification of quadrotor robot. *Abstract and Applied Analysis* 2014: 1–14.

Zheng EH, Xiong JJ and Luo JL (2014) Second order sliding mode control for a quadrotor UAV. *ISA Transactions* 55: 1350–1356.

Zuo Z (2010) Trajectory tracking control design with command-filtered compensation for a quadrotor. *IET Control Theory and Applications* 4: 2343–2355.